HHS Public Access

Author manuscript

Prog Lipid Res. Author manuscript; available in PMC 2017 April 01.

Published in final edited form as:

Prog Lipid Res. 2016 April ; 62: 1–24. doi:10.1016/j.plipres.2015.12.004.

Recent progress on lipid lateral heterogeneity in plasma membranes: from rafts to submicrometric domains

Mélanie Carquin[1,*], **Ludovic D'Auria**[2,*], **Hélène Pollet**[1], **Ernesto R. Bongarzone**[2], and **Donatienne Tyteca**[1]

[1] CELL Unit, de Duve Institute & Université Catholique de Louvain. UCL B1.75.05, Avenue Hippocrate, 75, B-1200 Brussels, Belgium.

[2] The Myelin Regeneration Group at the Dept. Anatomy & Cell Biology, College of Medicine, University of Illinois, Chicago. 808 S. Wood St. MC512. Chicago, IL. 60612. USA.

Abstract

The concept of transient nanometric domains known as lipid rafts has brought interest to reassess the validity of the Singer-Nicholson model of a fluid bilayer for cell membranes. However, this new view is still insufficient to explain the cellular control of surface lipid diversity or membrane deformability. During the past decade, the hypothesis that some lipids form large (submicrometric/mesoscale *vs* nanometric rafts) and stable (> min *vs* sec) membrane domains has emerged, largely based on indirect methods. Morphological evidence for stable submicrometric lipid domains, well-accepted for artificial and highly specialized biological membranes, was further reported for a variety of living cells from prokaryotes to yeast and mammalian cells. However, results remained questioned based on limitations of available fluorescent tools, use of poor lipid fixatives, and imaging artifacts due to non-resolved membrane projections. In this review, we will discuss recent evidence generated using powerful and innovative approaches such as lipid-specific toxin fragments that support the existence of submicrometric domains. We will integrate documented mechanisms involved in the formation and maintenance of these domains, and provide a perspective on their relevance on membrane deformability and regulation of membrane protein distribution.

Keywords

lipid domains; lipid probes; toxin fragments; living cells; membrane lipid composition; membrane deformability

Corresponding author: Donatienne Tyteca, CELL Unit, de Duve Institute & Université Catholique de Louvain, UCL B1.75.05, Avenue Hippocrate, 75, B-1200 Brussels, Belgium. Phone: +32-2-764.75.91; Fax: +32-2-764.75.43; donatienne.tyteca@uclouvain.be.

*Co-first authors

1. Introduction: key concepts and significance of lipid lateral heterogeneity

Even though the protein/lipid ratio of purified stripped membranes is close to the unity on a mass basis, their huge difference in molecular weight makes ~50 lipid molecules per membrane protein a reasonable general estimate, underlining that membrane lipids actually cover most of the plasma membrane (PM) [1, 2]. In addition, combinatorial variations in head-groups and aliphatic tails allow eukaryotic cells to synthesize thousands of different membrane lipids [3] by using ~5 % of their genes (for a review, see [4]). It seems reasonable that due to the intrinsic complexity of their lipids, cell membranes are arranged in far more intricate structures than simple homogenous fluid bilayers. Membrane heterogeneity is illustrated by unequal lipid distribution among (i) different PMs, (ii) distinct intracellular compartments, (iii) inner *vs* outer membrane leaflets, and (iv) the same leaflet. Whereas the three first levels of membrane heterogeneity are well accepted by the scientific community, the fourth level is still disputed. Limited availability of fluorescent tools, use of poor lipid fixatives, imaging of membrane artifacts, and description of unclassified membrane domains have intensified the debate in this rapidly growing area of research.

In this Section, we will provide a historical review of the different types of domains evidenced at the PM of eukaryotes. Current views on structural and dynamical aspects of biological membranes have been strongly influenced by the homogenous fluid mosaic model proposed by Singer and Nicolson in 1972 [5]. In this model, proteins are dispersed and individually embedded in a more or less randomly organized fluid lipid bilayer. In 1987, Simons and Van Meer discovered that glycosphingolipids (GSLs) cluster in the Golgi apparatus before being sorted to the apical surface of polarized epithelial cells [6]. In 1997, Simons and coll. proposed the lipid raft theory [7], where GSLs form detergent-resistant membranes (DRMs) enriched in cholesterol and glycosylphosphatidylinositol (GPI)-anchored proteins in cold non-ionic detergents such as Triton. Such theory was however questioned for several reasons. Among others, it has been shown that Triton can promote domain formation and may even create domains in a homogenous fluid lipid mixture, arguing against an identification of DRMs with functional rafts [8]. In 2006, lipid rafts were redefined as: “small (20-100nm), heterogeneous, highly dynamic, sterol- and sphingolipid (SL)-enriched domains that compartmentalize cellular processes. Small rafts can sometimes be stabilized to form larger platforms through protein-protein and protein-lipid interactions” [9]. In addition to rafts, other nanoscale domains, *i.e.* <100nm in diameter (also mis-called microdomains), have been described at the PM of eukaryotes: caveolae [10] and tetraspanin-rich domains [11]. Caveolae are defined as 60-80nm invaginations of the PM and are especially abundant in endothelial cells and adipocytes [12]. Tetraspanins are structural proteins bearing four transmembrane domains, which control the formation of membrane tubules. They can oligomerize and recruit various proteins to establish functional domains [13]. There are several reasons to consider lipid rafts, caveolae and tetraspanin-enriched domains as distinct types of domains (reviewed in [11, 14]). However, they share similarities such as small size, instability and governance by the liquid-ordered (Lo)/liquid-disordered (Ld) phase partitioning described in purified lipid systems (Section 2.1).

Besides nanometric lipid domains, morphological evidence for stable (min *vs* sec) submicrometric (*i.e.* >200nm in diameter *vs* 20-100nm) lipid domains was reported in

artificial [15-17] and highly specialized biological membranes, such as lung surfactant and skin stratum corneum [16, 18]. Such submicrometric domains, which are sometimes referred to as platforms, were first inferred in cells by dynamic studies [19-21]. However, morphological evidence was only occasionally reported and most of the time upon fixation [22-25]. In the past decade, owed to the development of new probes and new imaging methods, several groups have presented evidence for submicrometric domains in a variety of living cells from prokaryotes to yeast and mammalian cells [26-32]. Other examples include the large ceramide-containing domains formed upon degradation of sphingomyelin (SM) by sphingomyelinase (SMase) into ceramide (Cer) in response to stress [33-35].

However, despite the above morphological evidences for lipid rafts and submicrometric domains at PMs, their real existence is still debated. This can be explained by several reasons. First, lipid submicrometric domains have often been reported under non-physiological conditions. For example, they have been inferred on unfixed ghosts by high-resolution atomic force microscopy (AFM) upon cholesterol extraction by methyl-β-cyclodextrin [36]. Second, lipid or protein clustering into domains can be controlled by other mechanisms than cohesive interaction with Lo domains, thus not in line with the lipid phase behavior/raft hypothesis (see also Section 5). Kraft and coll. have recently found submicrometric hemagglutinin clusters at the PM of fibroblasts that are not enriched in cholesterol and not colocalized with SL domains found in these cells [37]. Likewise, whereas spatiotemporal heterogeneity of fluorescent lipid interaction has been found at the PM of living Ptk2 cells by the combination of super-resolution STED microscopy with scanning fluorescence correlation spectroscopy, authors have suggested alternative interactions than lipid-phase separation to explain their observation [38]. Third, other groups did not find any evidence for lipid domains in the PM. For example, using protein micropatterning combined with single-molecule tracking, Schutz and coll. have shown that GPI-anchored proteins do not reside in ordered domains at the PM of living cells [39].

Therefore, despite intense debates, plenty of lipid domains have been shown in the literature but their classification is still lacking. We propose to distinguish two classes of lipid domains, the lipid rafts and the submicrometric lipid domains, based on the following distinct features: (i) size (20-100nm *vs* >200nm); (ii) stability (sec *vs* min); and (iii) lipid enrichment (SLs and cholesterol *vs* several compositions, not restricted to SLs and cholesterol). Whether these two types of domains can coexist within the same PM or whether some submicrometric domains result from the clustering of small rafts under appropriate conditions, as proposed by Lingwood and Simons [40], are key open questions that must be addressed regarding biomechanical and biophysical properties of cell PMs. In addition, to clarify whether lipid domains can be generalized or not in biological membranes, it is crucial to use appropriate tools in combination with innovative imaging technologies and simple well-characterized cell models. In this review, we highlight the power of recent innovative approaches and modern imaging techniques. We further provide an integrated view on documented mechanisms that govern the formation and maintenance of submicrometric lipid domains and discuss their potential physiopathological relevance.

2. Lateral organization of lipids into submicrometric domains

2.1. Evidence in artificial systems and highly-specialized biological membranes

Model membrane systems have aided in understanding the lipid organization of cell membranes. Planar supported bilayers [41], giant unilamellar vesicles (GUVs) made from lipid mixtures [17, 42-44] as well as giant PM vesicles (GPMVs) [15, 16, 18, 45, 46] and PM spheres (PMS), distinct PM preparations segregated from the cytoskeleton and cytoplasmic content [15, 47], have provided elegant views to visualize membrane domains (Fig. 1). Planar supported bilayers represent model systems for exploring lipid domains by fluorescence microscopy or AFM (Section 3.2.4). The main advantage of planar supported bilayers to GUVs was for a long time related to their capacity to form asymmetric bilayers. However, a method to produce asymmetric GUVs was recently developed and validated by London and coll. [48]. Such vesicles exhibit asymmetric lipid distribution and size (~15-30μm in diameter) comparable to those of cell membranes, allowing thereby detailed microscopic analyses. The ability to control the membrane composition of GUVs is advantageous because it enables understanding the functional roles of specific lipids in the formation of domains. However, GUVs are less useful to extrapolate observations to systems with higher lipid compositional complexity such as the PM. Striking differences in lipid or protein partitioning can even be found between GUVs and GPMVs [49]. For more information on model membranes, please read [50].

Lateral membrane heterogeneity, with domains reaching several micrometers in diameter, is present in all of these model systems (Fig. 1). The shape is a particular feature of these domains reflecting differential phase coexistence and, hence, distinct lipid composition. Ld, Lo and solid-ordered phases (So; often called gel phase) are the most common phases found in artificial and biological membranes (for a review, see [35, 43]). Irregular shapes are observed in gel phases and usually found in pure systems of lipids with high melting temperature (T*m*) but generally poor in cholesterol [18, 44] (Fig. 1c,d). This contrasts with the smooth regular boundaries observed in liquid-phase coexistence [16, 17, 43, 47] (Fig. 1a,b,e).

To appreciate the possible phase states that can simultaneously exist in a membrane at thermodynamic equilibrium, one must consider the phase diagrams [51]. Each lipid species has an intrinsic temperature for physical transition from a solid- to a liquid-phase, known as the T*m*. Below the T*m*, membrane lipids are in solid- or gel-state structures. When the temperature is raised above the T*m*, the conformation of acyl chains changes, resulting into an increase of their disorder with more *gauche* conformation and, consequently, decreased packing. The Gibbs phase rule, which can only be applied if the lipid phases separate macroscopically, states that the number of de-mixed entities (P) for a system at equilibrium is correlated with the number of chemically independent components (C) by the following equation: P= C-F+2, where F is the number of independently variable intensive properties, such as temperature, pressure and mole fractions of phase components. Applying the Gibbs phase rule to a two-component system with a fixed composition and a fixed pressure, three phases can coexist at only one temperature, known as the triple point [51]. The situation is more complex in three-component systems, especially if they contain cholesterol, and in

biological membranes, consisting of thousands of different lipids. Thus, from the above equation, one may expect many different coexisting phases in biological membranes. However, this is not the case. As suggested by Lingwood and Simons, this could be explained by the fact that many PM components are not chemically independent but form specific complexes [40].

As mentioned above, fluorescence microscopy gives evidence for such micrometric separation in GUVs and in highly-specialized biological membranes, fitting into the classical description of phase separation by phase diagrams. The importance of temperature on micrometric membrane separation is illustrated with native pulmonary surfactant membranes in Fig. 2A [16]. Typical Lo/Ld-like phase coexistence can be observed at 36°C, while Ld domains show fluctuating borderlines at 37.5°C, and severe lateral structure changes with melting of most of the Lo phase occur at 38°C. Besides temperature, cholesterol and Cer are two lipids requiring a thorough consideration in the context of phase separation. Cholesterol is a key component of membrane biology and the concept of its clustering into membrane domains is attractive to explain its different functions including (i) membrane fluidity via lipid ordering; (ii) membrane deformability by modulation of PM protein interactions at the interface with cortical cytoskeleton [52]; (iii) formation and stabilization of nanometric lipid assemblies, rafts and caveolae [40, 53], as signaling platforms [54-56]; and (iv) phase coexistence in artificial membranes [57-59]. Fig. 2B shows the impact of modifying cholesterol concentration in GUVs formed from pulmonary surfactant lipid extracts. Partial cholesterol depletion (*i.e.* 10mol% instead of 20mol%) leads to elongated irregularly shaped domains, typical of gel/fluid phase coexistence. In contrast, increasing cholesterol content induces the appearance of circular-shaped domains, reflecting Lo/Ld phase coexistence (Fig. 2B [16]). Cer constitute the backbone of all complex SLs. Regarding their physico-chemical properties, Cer present very low polarity, are highly hydrophobic and display high gel-to-liquid-crystalline phase transition temperatures, well above the physiological temperature. These particular properties contribute to their in-plane phase separation into Cer-enriched domains. Hence, when mixed with other lipids, Cer can drastically modify membrane properties [60]. For instance, increase of Cer content induces the formation of micrometric domains with shape changes from circular to elongated forms (Fig. 2C [61]). These effects depend on Cer structure (*i.e.* acyl chain length and unsaturation), as well as on membrane lipid composition, particularly cholesterol levels. For a review on Cer biophysical properties, please see [60].

It should be noted that the formation of micrometric domains in artificial systems may not reflect the situation seen in biological membranes in which so many different lipids as well as intrinsic and extrinsic proteins are present. Thus, in cells, membrane lipid:protein interactions and membrane:cytoskeleton anchorage represent additional levels of regulation of lipid domain biogenesis and maintenance and are further discussed in Section 5.

2.2. Less straightforward evidence in plasma membranes

As shown in the previous Section, micrometric lipid domains are well-documented in artificial and highly specialized biological membranes. However, generalization of this concept to the plasma membrane of living cells is less straightforward and results have

remained doubted based on use of fluorescent tools (Section 2.2.1) and poor lipid fixatives (2.2.2) as well as imaging artifacts due to non-resolved membrane projections (2.2.3).

2.2.1. Use of fluorescent lipid probes—Whereas membrane labeling with fluorescent lipid probes represents a useful technique, it nevertheless presents the limitation that PM-inserted probes can differentially partition as compared to endogenous lipids, depending on membrane lipid composition and on the fluorophore [62]. To minimize artifacts, at least two criteria should be considered: (i) probe insertion at trace level within the PM, as compared with endogenous lipid composition, to ensure preservation of membrane integrity and avoidance of cell surface perturbations, and (ii) verification that the probe is a qualitative *bona fide* reporter of its endogenous lipid counterpart. After a short description of available fluorophores, we will briefly review the mostly used fluorescent lipid probes: (i) fluorescent lipid analogs bearing an extrinsic fluorescent reporter; (ii) intrinsically fluorescent lipids; (iii) fluorescent artificial lipid dyes; and (iv) small intrinsically fluorescent probes for endogenous lipids (Fig. 3a,b).

2.2.1.1. Fluorophore grafting: Except for intrinsically fluorescent molecules (see Sections 2.2.1.3, 2.2.1.4 and 2.2.1.5), it is generally required to covalently link molecules (lipids themselves or lipid-targeted specific proteins) to a fluorophore, in order to visualize membrane lipid organization. Among fluorophores, small organic dyes are generally opposed to big fluorescent proteins (EGFP, RFP, mCherry, Dronpa, *a.o.*). Most fluorophores used to label lipids are small organic dyes (Section 2.2.1.2) while both organic dyes and large fluorescent proteins are used to label lipid-targeted specific proteins (*e.g.* toxin fragments and proteins with phospholipid binding domain; see Sections 3.1.1 and 3.1.2).

Among others, major organic dyes developed so far to label lipids are 7-nitrobenz-2-oxa-1,3-diazol-4-yl (NBD) and 4,4-difluoro-5,7-dimethyl-4-bora-3a,4a-diaza-*s*-indacene (BODIPY). One can also cite the red-emitting Rhodamine dye KK114 or the Cy dyes. To label proteins, most commonly used fluorophores are Alexa Fluor, Atto or Cy dyes. Labeling kits based on amine- or thiol-reactive organic dyes are available. The labeling of the thiol group of cysteines is a more selective method than the amine-reactive approach, allowing a greater control of the conjugation because thiol groups are not as abundant as amines in most proteins.

While all organic dyes can be used in confocal microscopy, some dyes such as Alexa Fluor or Atto dyes have also been used to analyze living cells by super-resolution microscopy [63]. Indeed, such fluorophores have been shown to be reversibly photoswitched in the presence of thiol-containing reducing agents/thiol compounds. Interestingly, many organic dyes can be used in super-resolution microscopy under physiological conditions without additions [63, 64].

As compared to large fluorescent proteins, major advantages of organic fluorophores are (i) small size, preventing steric hindrance; (ii) possible labeling of one molecule with multiple fluorophores, enhancing the fluorescence signal [65]; and (iii) enhanced brightness and photostability [66]. Among drawbacks, one can cite (i) non-specific labeling to the targeted protein [67]; (ii) high labeling protein proportion which could cause fluorescence quenching

(depending on dye structure, charge and hydrophobicity) or prevent biomolecule function [65]; as well as (iii) higher background signal [67]. In conclusion, none of the fluorophores is “ideal”. In the meantime, a way to work is to compare the same lipid or protein molecule grafted with two unrelated fluorophores.

2.2.1.2. Insertion of fluorescent lipid analogs: Fluorescent lipid analogs are an attractive way to examine lipid membrane organization. Fluorophores can be linked either to lipid fatty acyl chains or to polar head-groups. Undoubtedly, the addition of fluorophores makes lipid analogs not equivalent to their endogenous counterpart. For instance, targeting modifications on the fatty acyl chain may perturb PM insertion, localization and/or phase behavior of the analog [68]. Importantly, this limitation can be minimized by the choice of a fluorophore which better preserve native phase partitioning, such as small and uncharged fluorophores like NBD or BODIPY [62]. NBD or BODIPY fluorescent lipid analogs present several advantages: (i) availability of numerous outer and inner PM lipid analogs; (ii) efficient delivery to cells with defatted bovine serum albumin (BSA) as a carrier molecule; (iii) possible extraction by „back-exchange’ using empty BSA; and (iv) a size close to their endogenous counterparts. Such analogs can be directly inserted in the PM but also used to metabolically label more complex lipids after incorporation of the fluorescent precursor. For example, NBD-Cer, a vital stain for the Golgi apparatus [69], can be converted into NBD-sphingomyelin (SM) in fibroblasts [70]. Similarly, cellular conversion of BODIPY-Cer into BODIPY-SM in CHO cells induces PM BODIPY-SM-enriched submicrometric domains, undistinguishable from those observed upon direct insertion of BODIPY-SM. This approach serves to rule out artifacts due to insertion of aggregates [30].

Although NBD-polar lipids have been widely used in the past, these probes present several disadvantages. First, NBD presents rapid photobleaching and is highly sensitive to its environment [71]. Second, NBD bound to fatty acyl chain “loops back” to the head-group region because of its polar nature [72]. BODIPY-polar lipids partially overcame the problems encountered with NBD-lipids. First, BODIPY displays significantly higher quantum yield and photostability than NBD [73], thus requiring insertion at lower concentration and imaging at lower laser power. Moreover, the insertion of BODIPY-lipids in membranes is deeper than that of NBD-analogs because of the higher hydrophobicity of BODIPY [74].

Regarding fluorescent sterols, the 22- and 25-NBD-cholesterol are available but their membrane orientation and/or distribution behavior have been shown to deviate from native cholesterol (for review, see [75]). Several BODIPY-cholesterol analogs have also been synthesized. However, these probes generally mis-partition, except when BODIPY is linked to carbon 24 (BODIPY-C24) of the sterol chain via the central dipyrromethene boron difluoride ring [75, 76]. A new derivative, where the fluorophore is bound via one of its pyrrole rings, shows superior behavior than BODIPY-C24-cholesterol, confirming the issue of the labeling position [77]. 6-dansyl-cholestanol allows depth insertion in fluid phase membranes and a distribution into cholesterol-rich *vs* -poor domains similar to that observed with native cholesterol [78-80]. However, this probe is highly photobleachable, restricting imaging time. Fluorescent polyethyleneglycol (PEG) cholesteryl esters represent another group of cholesterol probes, that differ from native cholesterol by their higher water

solubility, lack of hydroxyl group and main maintenance into the outer PM leaflet [39, 81]. As examples, one can cite the recently used fluorescein PEG-cholesterol (fPEG-chol) or the KK114 PEG-cholesterol (KK114-PEG-chol) [38, 39, 81].

2.2.1.3. Insertion of intrinsically fluorescent lipids: A few lipid probes such as dehydroergosterol (DHE) and the cholestatrienol are intrinsically fluorescent. These are generally preferred since they are not substituted by a fluorophore. The two main drawbacks of these analogs are their low quantum yield and their fast photobleaching, imposing membrane insertion at relatively high concentration. DHE, mainly synthesized by the yeast *Candida tropicalis* and by the single Red Sea sponge, *Biemna fortis* [82, 83], has been widely used (for review, see [75]). Structurally, DHE is similar to cholesterol, bearing three additional double bonds and an extra methyl group. Technically, it requires multiphoton excitation for live cell imaging and is not sensitive to the polarity of its environment. Its membrane orientation, dynamics and co-distribution with cholesterol in cells are faithful [84, 85]. For more information about applications and limitations of DHE in membrane biophysics and biology, see [75].

2.2.1.4. Insertion of artificial lipid probes: Lipidomimetic dyes, such as dialkylindocarbocyanine (DiI), diphenylhexatriene (DPH), Laurdan and aminonaphthylethenylpyridinium (ANEP)-containing dye (*e.g.* Di-4-ANEPPDHQ) families, are good alternatives for PM insertion. These probes do not mimic endogenous lipids but give information about the organization of the bilayer, such as membrane phase partitioning and fluidity. For details on DPH, Laurdan and Di-4-ANEPPDHQ, see [86-89]. DiI probes [59, 90, 91], known to be photostable [92], allow time-lapse and high-resolution imaging. This family includes several members that vary by their acyl chain length and unsaturation, influencing their membrane partitioning. Therefore, long chain DiI preferentially partition into the gel-like phase while shorter unsaturated DiI do so into the fluid phase [93].

2.2.1.5. Labeling of endogenous lipids by intrinsically fluorescent small molecules: Since insertion of exogenous lipids, even at trace levels, may perturb the organization of the host membrane, labeling of endogenous lipids by fluorescent small molecules will be generally preferred. Filipin is an example of such probes. Filipin was discovered in Philippine soil after isolation from the mycelium and culture filtrates of *Streptomyces filipinensis* [94]. This intrinsically fluorescent probe forms a complex with cholesterol or related sterols displaying a free 3'-OH group. Filipin is clinically used for the diagnosis of Niemann-Pick type C disease. However, this probe cannot distinguish between free or membrane-bound cholesterol and is highly cytotoxic, making it unsuitable for live cell imaging. Moreover, despite its wide use, it is unclear whether filipin faithfully reflects cholesterol distribution in membranes [95].

2.2.2. Poor membrane lipid fixation—Besides the choice of lipid probes and validation as *bona fide* qualitative tracers of endogenous counterparts (see above), it is also important to minimize other sources of misinterpretation. Fixation can be considered as a serious limitation because it can lead to artifactual lipid redistribution. Vital imaging techniques such as high-resolution confocal or scanning probe microscopy are recommended instead of

super-resolution or electron microscopy methods that generally require fixation (see Section 3.2). Of note, the fixation techniques used for fluorescence and electron microscopy are quite different. Formaldehyde is commonly used for fluorescence microscopy studies, including super-resolution, and is known to be reversible. The main drawbacks of such "light" fixation is its inability to cross-link lipids and to acutely arrest membrane protein long-range movement [96]. Conversely, for electron microscopy, samples are first fixed with glutaraldehyde (to irreversibly cross-link proteins), then post-fixed with osmium tetroxide (to cross-link lipids). This "hard" fixation has been shown to preserve the lipid bilayer [97], but its main drawback is the use of very toxic chemicals.

2.2.3. Limitation due to membrane projections—Another source of artifacts is related to PM projections. For instance, genuine lipid-enriched membrane domains can be easily confused with structural membrane projections such as filopodia, microvilli or ruffles, in which lipids are able to confine. This issue is especially relevant for cholesterol, known to preferentially associate with membrane ruffles [22, 98]. The use of flat membrane surfaces (*e.g.* the red blood cell, RBC) or mammalian nucleated cell membranes stripped of F-actin (to limit membrane ruffles) minimizes artifacts [29]. However, the latter approach can generate other difficulties due to lost interactions with the underlining cytoskeleton (see Section 5.2.2).

3. Evaluation of new tools and methods and importance of cell models

3.1. Tools

As highlighted in the previous Section, whereas the fluorescent lipid approach and labeling with filipin are attractive ways to examine lipid lateral heterogeneity, they present several limitations. It is thus essential to use more recent innovative approaches based on: (i) fluorescent toxin fragments (Section 3.1.1); (ii) fluorescent proteins with phospholipid binding domain (3.1.2); or (iii) antibodies, Fab fragments and nanobodies (3.1.3) (Fig. 3c-e; Table 1).

3.1.1. Fluorescent toxin fragments—Nature offers several toxins capable to bind to lipids, such as cholesterol-dependent cytolysins (Section 3.1.1.1), SM-specific toxins (3.1.1.2) or cholera toxin, which binds to the ganglioside GM1 (3.1.1.3). However, many of these proteins are pore-forming molecules and/or can induce artificial lipid clustering, considerably limiting their use. To overcome these limitations, non-toxic domain fragments or subunits of these toxins have been generated and coupled to fluorescent proteins (*e.g.* GFP, mCherry or Dronpa) or to organic fluorophores (*e.g.* Alexa Fluor) (Fig. 3c; Table 1). In order to define the best fluorophore to conjugate with the toxin fragment/subunit, please refer to Section 2.2.1.1.

3.1.1.1. Cholesterol-dependent cytolysins and non-toxic fragments: Cholesterol-dependent cytolysins are toxins specific to cholesterol produced by gram positive bacteria. Perfringolysin O (also named theta toxin), Streptolysin O and Listeriolysin O, produced by *Clostridium perfringens*, *Streptococcus pyogenes* and *Listeria monocytogenes,* respectively, are examples of available cytolysins. These toxins, which belong to the pore forming toxin

(PFT) group, self-associate into oligomeric pore-forming complexes after binding to cholesterol-containing membranes, thereby causing cytotoxicity. The theta toxin is one of the best characterized members of the family and is composed by four domains (D1-D4). D1 is the pore forming domain and D4 the minimal toxin fragment capable to bind to cholesterol with high affinity without causing lysis [99-102]. Binding of the two conserved amino acid residues (Thr490 and Leu491) of the D4 domain to the cholesterol hydroxyl group [101] induces configuration changes in the D1 domain, leading to theta oligomerization [103] and causing cell lysis [99]. To minimize cytotoxicity, toxin derivatives have been produced by two different approaches. In the first approach, a theta derivative, Cθ, was obtained by digestion with subtilisin Carlsberg prior to methylation (MCθ) or biotinylation (BCθ). BCθ is a suitable probe for cholesterol visualization and distribution [100, 104]. An alternative elegant approach is based on truncated theta, limited to its C-terminal domain D4 (theta-D4), fused with fluorescent proteins. Dronpa-theta-D4 is one of these derivatives best suited to super-resolution microscopy due to the reversible and switchable photoactivable Dronpa [22]. mCherry-theta-D4 is more photostable and suitable for vital confocal imaging [29]. In addition to general drawbacks of toxin fragments (see Section 3.1.1.4), a specific potential limitation of theta derivatives is that their binding to endogenous cholesterol is triggered only upon a certain cholesterol concentration threshold [105, 106]. For more information, see [107].

3.1.1.2. Sphingomyelin-binding toxins and non-toxic fragments: Lysenin and actinoporins, such equinatoxin II, are pore forming toxins capable to bind to SM. Lysenin is synthesized by the earthworm *Eisenia foetida* [108-110] and composed by a pore formation domain (amino acids 1-160) in the N-terminus and the SM-binding site (amino acids 161-297) in the C-terminus. Lysenin binding depends on local distribution and density of SM [108, 109, 111]. To overcome limitations due to oligomerization and/or pore formation, two approaches have been developed. The first approach is based on the observation that the C-terminus domain of lysenin is the minimal fragment responsible for specific SM binding without inducing oligomerization nor formation of membrane pores [24, 112]. Thus, a lysenin derivative has been developed, keeping only the C-terminus domain of the full lysenin. This derivative is generally named NT-lysenin (for Non-Toxic lysenin). In the second approach, a lysenin mutant based on substitution of tryptophan 20 by alanine was shown to fail in the formation of correct oligomers, resulting into loss of cytolytic activity but preserving ability to bind SM [113]. Such derivatives, coupled to fluorescent proteins (*e.g.* GFP, mCherry, mKate, Venus or Dronpa) or small organic molecules (*e.g.* Alexa Fluor), have proved useful in confocal or super-resolution microscopy analyses [22, 23, 26, 114] (see Table 1). For further general information on lysenin, please see [110, 111, 115]. Regarding equinatoxin II, produced from the sea anemone *Actinia equine*, the full-length toxin has been fused to fluorescent proteins in order to analyze SM distribution in cell membranes. Hence, to overcome limitation due to toxicity, a non-toxic equinatoxin II fragment (EqtII(8-69)) has proved useful (Table 1; Fig. 4d). In contrast to lysenin, known to bind clustered SM, equinatoxin II preferentially binds dispersed SM [114].

3.1.1.3. GM1-binding cholera toxin and non-toxic B subunit: Cholera toxin, secreted by gram-negative *Vibrio cholera* bacteria, is a multi-complex protein composed of two subunits,

the toxic A subunit and the non-toxic pentameric B subunit. In cholera, infection with this vibrio leads to sustained diarrhea after disruption of the epithelial barrier in intestinal enterocytes. The mechanism of this process involves the specific binding of the B subunit (CTxB) to GM1 ganglioside at the enterocyte PM [116, 117]. Despite the pentameric binding of CTxB to GM1 and its large size, the non-toxic CTxB has been successfully used to bind to GM1 without cellular toxicity, constituting an interesting and viable approach to analyze endogenous lipid organization. Each monomer of the pentameric CTxB has one binding site, thus CTxB is able to bind up to five GM1. Based on a multistep model, flow cytometry has shown that the affinity of a monovalent GM1-CTxB interaction is ~400-fold weaker than the one observed for the pentavalent interaction [118].

3.1.1.4. Advantages and drawbacks of plasma membrane labeling with toxin fragments/subunits: The use of toxin fragments/subunits to decorate endogenous membrane lipids offers several general advantages as compared to insertion of exogenous fluorescent lipid analogs: (i) targeting of endogenous lipids with high specificity; (ii) versatile coupling with fluorescent proteins or organic dyes; and (iii) possibility of probe radio-iodination for quantitative measurements [26, 29, 106]. Moreover, in contrast to filipin, toxin fragments/subunits can be used for live cell imaging. However, such probes present some drawbacks, such as (i) few number of specific toxin fragments produced and validated; (ii) recognition and binding limited to outer PM leaflet lipids; (iii) larger size than the targeted lipid and/or multivalence, with predicted steric hindrance of the toxin (see below); and (iv) prevention of native protein binding to the toxin targeted lipid, which could potentially affect biological function.

A critical feature to take into consideration regarding PM labeling with toxin fragments/subunits is their size and potential multivalence. In this respect, one must distinguish toxin fragments (*e.g.* theta and lysenin derivatives) and multimeric toxin subunits (*e.g.* cholera toxin B subunit). The multivalence and large size of the latter could induce changes in membrane properties and biochemical response. For instance, cross-linking of GM1 by the pentameric CTxB has been shown to induce changes in membrane phase behavior: in GUVs exhibiting one phase, addition and binding of CTxB induce lipid reorganization into coexisting fluid phases whatever the membrane was initially in Lo or Ld phase. Such phase separation was not due to CTxB self-aggregation but rather caused by GM1 cross-linking [119]. It should be however noted that this observation has been obtained in model membranes with defined lipid composition, devoid of proteins and cytoskeleton. Among other multimeric toxin fragments, one can also mention another member of the two-component toxin family, the Shiga toxin. The Shiga toxin B subunit is pentameric and each monomer has three binding sites to the glycosphingolipid globotriaosylceramide Gb3. Such toxin fragment, able to bind up to 15 Gb3, is not suitable to study lipid distribution. Accordingly, it has been demonstrated that addition of Shiga toxin B subunit induces changes in domain size and shape as well as lipid orientation in model membranes containing 1% Gb3 at a temperature above the phase transition [120].

In contrast, toxin fragments, such as theta or lysenin derivatives, are presumably monomeric due to removal of the domain involved in toxin oligomerization (Sections 3.1.1.1 and 3.1.1.2). Regarding the interference of the probe size, we expect a minor, if any, perturbation

on lipid binding specificity and on lipid membrane organization. Indeed, we recently demonstrated binding specificity of lysenin and theta fragments, with size much larger than endogenous lipids (~40kDa *vs* ~300-800Da), using defined-composition liposomes [26, 29]. Such experiment suggested that steric hindrance of the probe does not prevent binding specificity. Moreover, we have shown by double labeling experiment at the RBC PM that non-saturating concentration of the large lysenin toxin fragment (~45kDa; projected diameter ~15 times larger than endogenous SM) reveals the same submicrometric domains as upon insertion of BODIPY-SM (with a size similar to SM), independently from the order of labeling [26]. These data suggest that lysenin fragment does not trigger but rather reveals membrane organization into SM-enriched submicrometric domains. Likewise, the use of EGF-ferritin (~450kDa ferritin moiety) has been validated to authentically mimic 75-fold smaller EGF molecule [121]. Whereas minor perturbations are expected on binding specificity, the large probe size could nevertheless affect lipid properties such as lateral diffusion. This has been evidenced by fluorescence recovery after photobleaching (FRAP) of submicrometric domains at the RBC PM labeled by lysenin fragment and BODIPY-SM: the fluorescence recovery is thrice slower for toxin fragment as compared to BODIPY-SM, a difference that could be attributed to the larger size and/or steric hindrance of the toxin probe [26].

3.1.2. Fluorescent proteins with phospholipid binding domain—Besides toxin fragments, other probes are based on protein domains able to bind endogenous phospholipids. These can be either (i) expressed in the cytosol, being then able to bind inner PM phospholipids as well as cytoplasmic membranes of organelles (Fig. 3d; Table 1); and/or (ii) incubated with cells to target outer leaflet phospholipids after transbilayer flip-flop. The pleckstrin homology (PH) domain is one of these well-characterized probes specific for phosphoinositides (PIs; [122]). The ~100 amino acid-PH domain is contained in several proteins, such as pleckstrin or phospholipase C (PLC), with distinct binding affinity for different PIs [123]. For instance, PH domain of PLCδ (PH-PLCδ) has a high affinity for phosphatidylinositol-4,5-bisphosphate (PIP_2) [124, 125]. The discoidin C2 domain is another probe, specific for phosphatidylserine (PS). The ~160 amino acid-discoidin C2 domain is present in blood coagulation factors V and VIII, milk fat globule-EGF factor 8 (MFGE8; also known as lactadherin [Lact-C2]) and other plasma proteins. PH or discoidin C2 domains can be fluorescently tagged, allowing to study phospholipid membrane distribution [126-128]. Other globular domains capable to bind phospholipids at the membrane surface include: (i) the FYVE zinc finger domain found in EEA1 (Early Endosome Antigen 1) *a.o.* that binds to phosphatidylinositol-3-phosphate (PI3P); and (ii) the calcium-dependent phospholipid binding Annexins, such as Annexin A2, which preferentially interacts with PIP_2, or Annexin A5, which is currently the most commonly used probe for PS targeting at outer PM leaflet [129]. To further overcome limitation due to lack of PS labeling at the luminal membrane leaflet of organelles. Parton and coll. recently developed a novel on-section labeling approach on fast-frozen sample using purified GST (glutathione-S-transferase)-Lact-C2 fusion protein followed by transmission electron microscopy. This technique is based on high-pressure freezing, freeze-substitution with minimal fixatives and embedding at low temperature. Sections are then fixed, labeled with purified GST-Lact-C2 and followed by detection with anti-GST antibody and protein A–

gold. Such method avoids cell permeabilization as well as detergent extraction [126]. For more details on phospholipid-binding domains, please refer to [130]. Similarly to other probes, this approach also presents limitations including perturbation of normal lipid function upon high expression and high variability of affinity and specificity [129, 131].

3.1.3. Antibodies, Fab fragments and nanobodies—Antibodies have been recognized as gold standard to detect proteins. Interestingly, several antibodies have also been generated to decorate PM lipids (Fig. 3e). For example, there are monoclonal antibodies (mAbs) produced to detect specific GSLs expressed during the differentiation of oligodendrocytes and used for studying their *in vitro* maturation: (i) the mAb A2B5, against gangliosides GD3, GT3 and O-acetylated GT3 in early oligodendrocyte progenitors; (ii) the mAb O4, against sulfated GSLs expressed by late progenitors; and (iii) the mAb O1 and the mAb Ranscht, against galactosylceramides in mature oligodendrocytes (for a review, see [132]). These antibodies have revealed submicrometric GSL-enriched domains at different stages of oligodendrocyte differentiation, as illustrated in Table 1. Although less developed, antibodies are also used to decorate phospholipids. For example, the role of PS domains as targets for therapeutic treatment of viral infection has been highlighted by using a chimeric antibody that recognizes PS bound to membrane glycoproteins (mAb 3G4) [133]. Recently, phosphatidylcholine (PC) enrichment in neuronal structures has been revealed by an antibody against PC (mAb #15) [134]. These examples illustrate that antibodies can be useful to study membrane organization into submicrometric domains (see Table 1).

However, one must remain cautious of the drawbacks of antibodies since they require fixation (see Section 2.2.2), occasionally permeabilization and can exhibit multivalence leading to patching [135]. To overcome these issues, it is preferable to use fragments that do not create patching. One method is based on antibodies hydrolyzed into Fab fragments [136]. To the best of our knowledge, there is still no study using fluorescently labeled Fab fragments directed against lipids to study membrane organization. However, primary antibodies against galactosylceramide followed by fluorescent secondary Fab fragments have revealed submicrometric domains in oligodendrocytes induced by co-culture with neurons, ruling out that domains were induced by crosslinking of secondary antibodies [137]. An alternative approach would be to exploit the derivatives of *Camelidae* antibodies. Unlike conventional antibodies which are made of heavy and light chains, the antibodies from *Camelidae* are only composed of two identical heavy chains, each being fully capable of binding independently the affiliated antigen. The advantages of isolating single heavy chain fragments from *Camelidae*, also called nano-antibodies or nanobodies™, rely upon their small size as compared to Fab fragments (~15 *vs* ~55kDa, respectively) that can reach confined areas inaccessible to larger probes [138]. Such nanobodies have been developed for epithelial growth factor receptor, allowing to evidence a cholesterol-independent colocalization of the receptor with GM1 ganglioside [139]. However, there is still a lack of studies using nanobodies to detect submicrometric lipid domains. Nevertheless, the generation of fluorescently conjugated Fab fragments or nanobodies against lipids could in the future become an interesting strategy for analyzing membrane lipid organization.

3.2. Methods

The low imaging resolution, combined with the poor preservation of lipid organization upon fixation (see Section 2.2.2), has been a major limitation for studying the dynamic compartmentalization of lipid species in cells. The advent of improved imaging technologies has provided the opportunity to rectify these constraints and learn about lipid domain morphology and dynamics in cells. This section gives a brief and non-exhaustive overview of modern microscopy techniques with their advantages and limitations in the context of lipid organization into submicrometric domains (Table 2). The Table also lists selected reviews to which the reader can refer for an in-depth information about techniques. Moreover, selected techniques are illustrated in Figs. 4-7.

3.2.1. High-resolution confocal microscopy and related techniques—

Contemporary microscopy has evolved from whole-cell visualization to high-resolution microscopy that can discriminate objects down to the diffraction limit of ~200nm at the X-Y axis and are widely used for live cell imaging. Three representatives of high-resolution microscopy are (i) conventional confocal imaging, (ii) two-photon excitation microscopy and (iii) Total Internal Reflection Fluorescence (TIRF). Confocal scanning has allowed to set forth submicrometric lipid domains in several cells [26, 27, 29, 30, 140-142]. Two-photon microscopy has proven very useful to examine membrane organization on artificial systems (for a review, see [43]) but also on living cells, especially by using UV-excited probes, such as dehydroergosterol (DHE) [143] or Laurdan [144] (see Section 2.2.1). TIRF microscopy has mainly been used to visualize membrane proteins. Nevertheless, this technique is also developed to determine lipid organization. As an example, one can cite the visualization of GM1 distribution on HEK293T cells labeled with CTxB (Fig. 4a; Table 1) [145].

Optical microscopy is a versatile tool that can generate mapping of structures but also provide information about properties and interactions of these structures. Fluorescence Recovery After Photobleaching (FRAP) can be adapted to confocal microscopy and can determine kinetic properties of fluorescently labeled membrane components by taking advantage of tracking molecules in live cell imaging after photobleaching. The use of different beam radii for photobleaching fluorescent lipid analogs has allowed to infer the existence of submicrometric lipid domains [19, 30, 146]. Fluorescence Lifetime Imaging Microscopy (FLIM) has been used to detect submicrometric domains in Laurdan-labeled NIH 3T3 fibroblasts or upon RBC infection by *Plasmodium falciparum,* which creates areas of cholesterol heterogeneity [147, 148]. Fluorescence Correlation Spectroscopy (FCS) can determine molecular concentration, diffusion as well as intra- and inter-molecular interactions. By comparison of diffusion coefficients of lipid analogs at the outer PM, this technique has allowed to evidence submicrometric domains [149, 150].

Together, these widely used techniques provide complementary tools for detection of submicrometric lipid domains in living cells. However, their major limitations rest upon the use of exogenous markers (*e.g.* fluorescent lipid analogs) and the resolution of domains that is constrained by the optical diffraction limit (~200nm). Specific advantages and drawbacks of all these techniques for studying lipid organization are summarized in Table 2.

3.2.2. Super-resolution microscopy—Recently, major breakthroughs in the field of light microscopy have overcome the diffraction limit, resolving structures separated by a distance smaller than 200nm. This leads to a new field of investigation for mapping membrane structures, the super-resolution microscopy. Interestingly, several techniques of super-resolution microscopy have not only resolved structures of a few nanometers in diameter but have also revealed or confirmed the existence of submicrometric lipid domains. Photo-Activation Localization Microscopy (PALM) and Stochastic Optical Reconstruction Microscopy (STORM) use photoswitchable fluorescent probes to reveal spatial differences between molecules. The seminal work on lipid organization using super-resolution on HeLa cells has revealed SM and cholesterol clusters of ~250nm in diameter (Fig. 4b) [22]. Thanks to Structured Illumination Microscopy (SIM), Makino and coll. have evidenced dispersed and clustered pools of SM at the apical PM of pig kidney epithelial cells labeled by two SM-specific toxins (Fig. 4c) [114]. Single Dye Tracing (SDT) allows to analyze diffusion properties of a single labeled molecule. Upon insertion of fluorescent analogs of saturated and unsaturated phospholipids in human airway smooth muscle cells, SDT has revealed submicrometric clusters of saturated lipids (Fig. 4d), which diffuse more rapidly but in a unidirectional way. The study also showed that submicrometric domains maintain their position, suggesting the influence of the underlining cytoskeleton on lipid partitioning [21], as proposed by other studies.

Nevertheless, it should be noticed that, despite the recent wealth of information gained, these techniques have the inherent disadvantages that they require the use of exogenous probes and that they are so far difficult to apply to living cells due to phototoxicity and photobleaching. Excited fluorophores produce reactive oxygen species which react with a large variety of easily oxidizable components, such as proteins, nucleic acids, lipids and fluorophores, leading to loss of fluorescence signal (photobleaching) and cell cycle arrest or cell death (phototoxicity). An additional major difficulty for application of super-resolution microscopy on live cells is the mobility of the labelled molecule, which leads to substantial blur during the overall recording time.

3.2.3. Secondary Ion Mass Spectroscopy—Secondary Ion Mass Spectrometry (SIMS) allows direct imaging of membrane structures at a very high resolution (50-100nm) by combining mass spectrometry molecule identification with imaging. Thanks to this technique, Kraft and coll. have discovered SL-enriched submicrometric domains at the fibroblast PM after metabolic labeling with ^{15}N-SL precursors (Fig. 4e) [25, 151].

This technique presents the main advantage of studying directly endogenous lipids by metabolic labeling with isotopes, which drastically decreases the risk of distribution artifact that can be encountered with fluorescent lipid probes or antibodies.

3.2.4. Scanning probe microscopy—Atomic Force Microscopy (AFM) is a high-resolution scanning probe microscopy, detecting differences in roughness at the nanometer scale. Among others, this technique has revealed submicrometric domains on (i) the RBC membrane upon cholesterol depletion (Fig. 4f) [36]; (ii) the external membrane leaflet of kidney brush-border membrane models [152]; and (iii) membrane purified by ultracentrifugation from human breast cancer cells (MDA-MB-231) [153]. AFM has become

extremely advanced by a multiparametric analysis of samples by combining super-resolution imaging, topography, molecular interactions and mechanical measurement [154]. A related method is Near-Field Scanning Optical Microscopy (NSOM) with a resolution that can reach ~20nm [155]. NSOM has revealed clustering of GM1 and GM3 in domains of ~40-360nm at the apical PM of epithelial cells [156].

3.3. Cell models

The complexity of the PM led scientists to work on model lipid bilayers with controlled and simple composition. These models include supported bilayers and large vesicles such as GUVs or GPMVs (reviewed in [157]; see also Section 2.1). Even if these models have greatly helped to understand the properties of lipid bilayers, these do not authentically reflect biological membranes, including the diversity of membrane lipid and protein composition, the complexity of lateral and transversal lipid asymmetries and the influence of the cytoskeleton on membrane organization. Bacteria represent an alternative model to study membrane lipid organization. *E. coli* for example is very well characterized, grows rapidly and allows easy genetic manipulations, popular for functional studies. Nevertheless, bacteria are small (less than few μm) and require high-resolution microscopy to be properly analyzed. Moreover, the PM composition of prokaryotes is quite different from the mammalian PM (Table 3), leading to different organization and functions. Yeast represents another powerful model to investigate membrane lipid organization and especially the importance of proteins in this process. *Saccharomyces Cerevisiae* is one of the most intensively used eukaryotic models due to comprehensive banks of mutants, a size (~10μm) compatible with conventional microscopy and a rapid growth. However, the yeast cell wall limits penetration of molecules larger than ~700Da [158], preventing incorporation into intact yeast of fluorescent analogs of polar lipids mixed with BSA as lipid carriers. Other labeling approaches, such as expression of lipid specific markers, have to be developed to circumvent this difficulty (see Section 3.1.2). Mammalian nucleated cells offer the possibility of co- and 3D-culture and an easy growth. However, they usually present considerable limitations to study membrane lipid lateral organization due to lipid metabolism, endocytosis and a tortuous surface due to vesicular trafficking and membrane protrusions, which can lead to false interpretations. This is why our group focuses on RBCs [26, 27, 29, 30, 146]. RBC is the simplest and best characterized eukaryotic cell system, both at lipid and protein levels [159, 160]. Moreover, for practical purposes, RBCs (i) are easily available and robust; (ii) are highly homogenous in size and shape due to rapid clearance of damaged RBCs by the spleen; (iii) present a flat surface without membrane projections or protrusions, avoiding confusion between domains and lipid enrichment in membrane ruffles; (iv) do not metabolize lipids; and (v) do not make endocytosis, avoiding any confusion between domains and endosomes.

Whereas all membranes described above represent interesting models to visualize lipid organization, it has to be kept in mind that their composition is quite different. Table 3 gives the PM composition of different cell types. For instance, SM and cholesterol contents of the RBC PM are particularly high, as compared to the PM of human alveolar macrophages. Since cholesterol plays a dominant role in the regulation of membrane fluidity, changes in cholesterol levels will differentially modulate membrane organization into domains in these

PMs. It is also important to note that yeast PM exhibits ergosterol instead of cholesterol, while most bacteria PMs do not contain sterols. Other factors such as the PM anchorage to the underlying cytoskeleton, which is about 20-fold stronger in RBC than in fibroblasts, and the presence of a cell wall, as in yeast, should also be considered (see Section 5.2). Therefore, generalized discussions of submicrometric membrane domains need to be done cautiously within the context of PM compositional heterogeneity and membrane anchorage to the cytoskeleton.

4. Direct evidence for submicrometric lipid domains in living cells

In 1987, Yechiel and Edidin suggested the existence of submicrometric domains [19]. Their discussion arose from FRAP analysis at various sizes of photobleached spots on human skin fibroblasts, using a fluorescent PC analog. The morphological evidence was less convincing due to the imaging capacity available at the time. In 1991, Rodgers and Glaser visualized submicrometric domains on erythrocyte ghosts after insertion of fluorescent phospholipid analogs, without clear equivalents found in living RBCs [20]. In 2002, Kusumi and coll. hypothesized that phospholipids are confined within compartments delineated by transmembrane proteins anchored to the underlying cytoskeleton and acting as pickets, before undergoing hop diffusion to adjacent compartments ([21]; see also Section 5.2). In the past decade, several groups have presented evidence of submicrometric domains in a variety of living cells, including prokaryotes (Section 4.1), yeast (4.2) and animal cells (4.3), although some generalizations appear still premature.

4.1. Prokaryotes

The existence of nanometric lipid domains has been for a long time restricted to eukaryotes simply because their formation and/or maintenance require sterols, which are absent from the membranes of most bacteria (see membrane composition of *E. coli* at Table 3). However, it has been recently shown that bacteria organize many signal transduction, protein secretion and transport processes in functional membrane microdomains, which seem equivalent to eukaryotic lipid rafts (reviewed in [161]). The formation of these functional membrane microdomains seems to require flotillin-like proteins. Interestingly, heterogeneous distribution in domains of a flotillin-like protein from *B. Subtilis* has been directly visualized by fluorescence microscopy [162]. The importance of flotillins was further highlighted by the observation that domains exhibiting high GP value in Laurdan-labeled *B. subtilis* (Fig. 5a) could coalesce into larger domains upon loss of flotillins [31]. However, lipid composition of these flotillin-enriched structures is not clear. Since sterols are absent from most bacterial membranes, domain organization should depend on sterol surrogates and, hence, the involvement of polyisoprenoid lipids has been proposed (reviewed in [161]). A recent study using nanoSIMS has suggested hopanoid (pentacyclic triterpenoids structurally similar to steroids)-enriched domains in cyanobacterium *Nostoc punctiforme* [163].

Using the fluorescent dye 10-N-nonylacridine orange (NAO) that decorates cardiolipin, other groups have shown the presence of cardiolipin-enriched domains at the cell poles and at the division septum in *E. coli* [164] and *B. subtilis* [165], suggesting the presence in bacterial membranes of domains that could be involved in cell division. Whether functional

membrane microdomains and cardiolipin-enriched domains are spatially and functionally related remains to be explored. Importantly, it is also still unclear if bacterial and eukaryotic membrane domains share similarities. Taking into account the resolution limits of available microscopy techniques, this question is particularly difficult because of the small size of bacteria (sometimes less than 1μm) and domains.

4.2. Yeast

Yeast represents a powerful system to explore PM lipid and protein organization based on genetic approaches. The PM of *S. cerevisiae* is known to be organized as a patchwork of several protein domains [128]. Regarding lipid organization, studies using filipin have shown that the budding yeast PM contains ergosterol-enriched domains (Fig. 5b) that colocalize with the protein Sur7, a protein found in eisosomes [32]. Network-like lipid domains have also been shown at the cytosolic PM leaflet, by targeting PS and PIP_2 with Lact-C2 and PH domains [128] (see Section 3.1.2). More recently, major redistribution of PIP_2 into enriched membrane clusters upon osmotic stress has been clearly evidenced for both fission and budding yeast cells [166, 167]. Such PIP_2 clusters are spatially organized by eisosomes, protein-based structures of the yeast PM which regulate activation of MAPK signal transduction through the organization of cortical lipid-based domains [166]. Interestingly, after perturbation of SL, sterol, PS or PIP_2 levels, patchwork protein distribution is modified [128], suggesting a relation between proteins and lipids at the yeast PM domains. For more information of this subject, please see [168, 169].

In addition, other groups have suggested the existence of gel-like domains in yeast, but with no morphological evidence and thus no domain size estimation. For instance, fluorescence intensity and anisotropy decay analyses using *trans*-Parinaric acid (t-PnA) or 1,6-diphenyl-1,3,5-hexatriene (DPH) show reduced lateral heterogeneity in gel-like domains in yeast with low SL levels, suggesting an essential role of SLs in these domains [170, 171].

4.3. Animal cells

As mentioned in the Introduction Section, submicrometric lipid domains have sometimes been reported under non-physiological conditions, leading to intensified debate on their real existence in physiological conditions. For instance, submicrometric domains have been visualized in RBCs after alteration of membrane Cer and cholesterol contents upon treatment with PlcHR2, a toxin from *Pseudomonas aeruginosa* exhibiting both phospholipase C and SMase activities [172], or methyl-β-cyclodextrin [36], respectively. A similar example was generated using CHO cells depleted of cholesterol [173]. Moreover, there are cases in which submicrometric domains have not been detected. Thus, whereas submicrometric domains enriched in SLs have been detected by SIMS at the fibroblast PM, cholesterol is uniformly distributed throughout [25, 151]. Likewise, using protein micropatterning combined with single-molecule tracking, Schutz and coll. have shown that GPI-anchored proteins do not reside in ordered domains at the PM of living cells [39].

However, lipid domains have been documented in other cases with reliable approaches. These were identified at the outer and/or inner PM leaflet of various cell types, using different tools and methods. A substantial, albeit non-exhaustive, list of examples is

presented in Table 1 and representative vital confocal images are shown in Fig. 5c-f. Our group focuses on human RBCs as a model of choice for the reasons mentioned at Section 3.3. Thus, by vital confocal imaging of RBCs partially spread onto poly-L-lysine-coated coverslips, trace insertion in the outer PM leaflet of fluorescent lipid analogs has revealed submicrometric domains of ~0.5μm in diameter. Similar domains have been observed upon direct labeling of endogenous SM and cholesterol using toxin derivatives (Fig. 6, 7 & Table 1) [26, 27, 29, 30, 146]. Importantly, double labeling of RBCs with the SM-specific lysenin fragment (see above), then with BODIPY-SM, reveals perfect colocalization, suggesting the relevance of BODIPY-SM to study its native counterpart [26]. Submicrometric lipid domains have been confirmed on RBCs suspended in a 3D-gel, thus without artificial stretching, suggesting a genuine feature of RBCs *in vivo.* Mechanistically, lipid domains are governed by temperature, membrane lipid composition and membrane:cytoskeleton anchorage, thus by membrane tension (Fig. 7; see also Section 5) [26, 29].

In addition to RBCs, oligodendrocytes are also a useful model to study PM organization, based on differential relative abundance of specific lipids during differentiation (Section 3.1.3; for a review, see [132]) and a high global lipid content (~75% of their total dry weight, with a protein:lipid ratio of ~0.3 *vs* ~1 in most cells [174]). In fact, several reports have contributed with seminal findings in this regard. First, PIP_2 is a major regulator of myelin compaction by its close interaction with myelin basic proteins [175]. Second, galactosylceramide and sulfatides form submicrometric domains [176], mutually interacting at the apposed membranes of wrapped myelin (for a review, see [177]), regulating PM organization and lateral diffusion of myelin proteins [178]. Third, GM1 submicrometric domains are essential for oligodendrocyte precursor survival by providing signaling platforms for growth factor-mediated integrin activation [179]. Fourth, sulfatide submicrometric domains are necessary for neuron-dependent oligodendrocyte maturation by contact with laminin, a molecule that is present at the axolemma [180] (Table 1).

Lipid domains can also be generated by the hydrolysis of specific lipids. As an example, one can cite the Cer-rich domains with diameters of 200nm up to several micrometers that can be formed upon degradation by acid SMase of sphingomyelin into Cer in response to stress [33-35]. Such domains, also called platforms, can be visualized by a variety of techniques, including fluorescence and confocal microscopy, and exhibit a gel like phase. They can play a role in transmembrane signaling and can be involved in the physiopathology of various diseases, including cancer [34].

5. Biogenesis

It is not clear how submicrometric lipid domains are formed, but various mechanisms have been proposed. These include: (i) lipid:lipid interactions (Section 5.1); (ii) protein:lipid interactions, including with the cytoskeleton or the cell wall (5.2); (iii) membrane turnover (5.3); and (iv) extrinsic factors such as temperature, pH and osmolarity (5.4). Interplay/ balance between these different mechanisms likely varies from one cell to another, impacting on domain abundance, size (Section 4) and function (Section 6).

5.1. Lipid-based mechanisms

Artificial models are convenient to analyze biophysical parameters of lipid domains and have been at the cornerstone of identifying key regulators of lipid submicrometric domains in biological membranes (for reviews, please see [181-184]). These include cholesterol, complex SLs and Cer, *a.o.*. Cholesterol is the most abundant lipid in several PMs, with up to ~45mol% in RBCs (see Table 3). This lipid emerges as a major regulator of submicrometric domain biogenesis and/or maintenance in living cells, as illustrated by the following studies. Depletion of cholesterol from living fibroblasts or CHO cells labeled by fluorescent SM analogs induces the formation of submicrometric domains or increases their size, indicating a restricting role of cholesterol for domain formation/maintenance in these cells [30, 173]. In contrast, slight cholesterol depletion of the RBC PM decreases the abundance of PC- and SM- but not GSLs-enriched submicrometric domains [26, 27] as well as lipid packing, as revealed by Laurdan [185]. Moreover, cholesterol influences the shape of submicrometric domains. For example, lowering cholesterol levels in native pulmonary surfactant membranes induces a transition from circular to fluctuating borderline micrometric domains, typical of gel-ordered like phases [16]. The fine and ambivalent effect of cholesterol on submicrometric domains in different cells may be related to differences in membrane composition. Indeed, cholesterol has been proposed to either promote lipid mixing by converting gel and Ld phases into an intermediate Lo phase or, conversely, to favor SL coalescence into SL- and cholesterol-rich Lo domains that separate from Ld domains [186].

Supporting the importance of SLs for domain organization, we have shown that cholesterol-enriched submicrometric domains at the PM of RBCs are abrogated by SM depletion [29] (Fig. 7b). Takamori and coll. showed that signal translation associated submicrometric domains are only formed in a neutrophil cell line expressing long fatty acyl chain lactosylceramide (LacCer) [187]. In line with this evidence, natural D-*erythro*-LacCer is more prone to form highly-enriched submicrometric domains than the artificial L-*threo*-LacCer [188]. These two studies suggest that both the fatty acyl chain length and the overall conformation of the SL play a role in domain formation and/or maintenance.

Whereas Cer levels are extremely low in resting PMs, Cer significantly increases in stress conditions and in response to stimuli by the hydrolytic action of SMase on SM, playing key roles in a variety of cellular processes and diseases ([60, 172]; see also Section 6.4). Interestingly, the extent of Cer-induced alterations is influenced by the interplay between cholesterol and SM ratios: Cer-enriched domains are formed in conditions with low but not high cholesterol levels. For more details, please see [60].

Depending on their lipid composition (especially cholesterol, SL and Cer contents), lipid domain biophysical properties can strongly vary. Among others, one can cite: (i) membrane fluidity, a property highly influenced by the nature of lipids and the degree of unsaturation of fatty acyl chains; (ii) membrane asymmetry resulting from differences in composition of the two membrane leaflets and the slight area excess in the outer layer (bilayer couple hypothesis) [189]; and (iii) membrane curvature and the bending energy due to the resultant bilayer rigidity and the line tension on domain edges [190, 191].

5.2. Protein-based mechanisms

Lipid clustering in submicrometric domains not only arises from physical order, consequent from lipid acyl chains and sterol content (see Section 5.1), but also from specific chemical interactions between membrane proteins and lipids (Section 5.2.1). In addition, the cytoskeleton also influences lipid assembly (5.2.2). Other factors such as membrane turnover (5.2.3) and external factors (5.2.4) will also be briefly discussed.

5.2.1. Specific membrane protein:lipid interactions—Membrane association of a protein can be achieved by different ways. Membrane interaction can simply occur by a membrane-spanning region, which is hydrophobic and then preferentially localized in a layer of lipid molecules. The first shell of lipid molecules interacting directly with the protein is called the lipid annulus and is thought to be a set of lipid molecules which preferentially binds to the surface of the membrane protein. These interactions are weak and are driven by many van der Walls, hydrogen bonding and electrostatic interactions [192]. Even if these interactions are not very specific, they can play a cooperative role and modulate the protein function or localization. It is already well studied that the sarcoplasmic reticulum/endoplasmic reticulum calcium-ATPase (SERCA) activity is affected by the composition and structure of its lipid annulus [193]. Specific lipids of the bilayer can also directly interact with the transmembrane domain of the protein with stronger interactions. Case in point, the cytochrome c oxidase interacts specifically with thirteen lipid molecules among which four of them stabilize the homodimer formation [194]. A highly specific interaction between one SM species (C18:0) and a transmembrane domain has been shown in the protein p24, implicated in the COPI machinery from the Golgi. It seems that SM act here as cofactors and regulate the equilibrium between an inactive monomeric and an active oligomeric state of the p24 protein, allowing regulation of the COPI-dependent transport [195].

Besides integral membrane proteins, many soluble proteins can bind membrane bilayers via lipid-binding domains. For example, ERM proteins (Ezrin, Radixin, Moesin) mediate the anchorage of actin to the PM, via their PH-domain specific for PIP_2 [196, 197]. Protein kinase C can also bind to PM through a C1 domain specific for diacylglycerol (DAG) and is activated when the concentration of DAG is increased [130]. Whereas these domains generally have for target very specific and rare lipids that are known to be regulated in time and/or space, there are lipid-binding domains which recognize an abundant and ubiquitous phospholipid. For example, calcium-dependent C2 domains and Annexin A5 interact with PS only when the calcium concentration is high enough, allowing a regulation in time and/or space that the abundant target would not have [130]. Less specific interactions could occur between proteins and lipids via electrostatic interactions between polybasic sequences in the protein and acidic phospholipids in the inner PM leaflet. For example, clustering of syntaxin-1A, the major protein of the SNARE complex (Soluble N-ethylmaleimide-sensitive factor Attachment protein Receptor) can be induced by membrane enrichment in PIP_2 owed to its polybasic sequence [198]. However, these interactions are weak and PIP_2 can be released for example when the local intracellular calcium level increases, allowing another level of regulation [199].

Finally, proteins can be associated to the membrane by post-translational addition of lipid anchors, including (i) GPI anchors; (ii) myristic/palmitic acid tails; and (iii) isoprenylation [200]. GPI-anchored proteins are located to the extracellular PM leaflet while the others are on the cytoplasmic leaflet. Each one differs by the length and the saturation of the acyl chains. GPI-anchored and palmitoylated proteins have mostly long saturated acyl chains and are suspected to be associated with lipid rafts, while proteins bound to the membrane by isoprenyl and myristoyl anchors have shorter and/or unsaturated acyl chains that seem less clustered in membranes [201]. Moreover, such protein lipidations can be dynamically regulated. GPI-anchored proteins can be released from the membrane by the action of a PI-specific phospholipase C [202] and the membrane anchorage of myristoylated proteins can be activated by a “ligand”-dependent conformational change of the protein leading to exposure of the myristoyl moiety previously sequestered in the protein [203]. Palmitoylation is the only one which is reversible thanks to protein acylthioesterases responsible for the removal of the palmitate [204]. All these mechanisms may be relevant for spatial and temporal regulation of signaling and shaping events.

5.2.2. Interactions between the plasma membrane and the cortical cytoskeleton or the cell wall—The interaction between PM and the cortical actin cytoskeleton represents another important factor for lipid domain biogenesis/maintenance. By studying the movement of unsaturated phosphatidylethanolamine (PE) in rat fibroblasts, Kusumi and coll. suggested that the PM is compartmentalized into large areas (~750nm in diameter) containing smaller regions (~230nm in diameter). This appears to result from an actin-based membrane cytoskeleton fence structure with anchored transmembrane proteins acting as pickets [21]. Electron tomography reconstruction of the cytoskeleton:membrane interface revealed that the PM cytoskeleton covers the entire cytoplasmic surface in close association with clathrin coated pits and caveolea. This double compartmentalization model may explain the slower diffusion rate of lipids observed in cell membranes than that measured in artificial bilayers. A model for the PM organization into three domains of decreasing size and showing cooperative actions was subsequently proposed by Kusumi and coll. [205-207]: (i) the membrane compartment (40-300nm in diameter), corresponding to the PM partitioning mediated by the interactions with the actin-based membrane cytoskeleton (fence) and the transmembrane proteins anchored to the membrane cytoskeleton fence (pickets); (ii) the raft domains (2-20nm) confined by the anchored transmembrane proteins; and (iii) the dynamic protein complex domains (3-10nm), including dimers/oligomers and greater complexes of membrane-associated and integral membrane proteins. This model is supported by the demonstration by Frisz and coll. that actin depolymerization induces a randomization of ^{15}N-SLs in fibroblasts, indicating that SL-enriched domains strongly depend on the actin-based cytoskeleton [25]. More recently, Mayor and co-workers provided experimental and simulation data showing that nanoclustering of GPI-anchored proteins at the outer PM leaflet by dynamic cortical actin is made by the interdigitation and transbilayer coupling of long saturated acyl chains. Interestingly, authors also suggest that cholesterol can stabilize Lo domains over a length scale that is larger than the size of the immobilized cluster, supporting the importance of cholesterol in this process. This mechanism could have implications not only for the construction of signaling platforms but also for cell deformation in many physiopathological

events such as migration, possibly via the formation of the contractile actin clusters that would determine when and where domains may be stabilized [208] (see also Section 6.1).

These two studies contrast with the observation that acute membrane:cytoskeleton uncoupling in RBCs increases the abundance of lipid submicrometric domains (Fig. 7c) [29]. The reason for this difference could reside in that, contrarily to most animal and fungal cells with a cortical cytoskeleton made of actin filaments and slightly anchored to the membrane, the RBC cytoskeleton is primarily composed by spectrin and is more strongly anchored to the membrane (*e.g.* > 20-fold than in fibroblasts) [209].

Like RBCs, yeast exhibits membrane submicrometric domains with bigger size and higher stability than in most mammalian cells. These features could not be due to the cytoskeleton since yeast displays faster dynamics of cortical actin than most cells, reducing its participation in restricting PM lateral mobility [128]. They could instead be related to close contacts between the outer PM leaflet and the cell wall which impose lateral compartmentalization of the yeast PM (for details, see the review [169]). For instance, clustering of the integral protein Sur7 in domains at the PM of budding yeast depends on the interaction with the cell wall [210]. As an additional potential layer of regulation, the very close proximity between the inner PM and endomembrane compartments, such as vacuoles or endoplasmic reticulum, has been proposed to impose lateral compartmentalization in the yeast PM, but this hypothesis remains to be tested [169]. For molecular and physical mechanisms involved in lateral PM heterogeneity in yeast, please see [168, 169].

5.3. Membrane turnover

In eukaryotic cells, membrane lipid composition of distinct organelles is tightly controlled by different mechanisms, including vesicular trafficking (for a review, see [4]). This must feature be considered as an additional level of regulation of PM lateral organization in domains. There is a constant membrane lipid turnover from synthesis in specific organelles (*e.g.* endoplasmic reticulum, Golgi) to sending to specific membranes. One can cite the clustering of GSLs in the Golgi apparatus during synthesis before transport to and enrichment at the apical membrane of polarized epithelial cells [6]. Once at the PM, lipids can be internalized for either degradation or recycling back. This process called endocytosis is regulated by small proteins, such as Rab GTPases, that catalyze the directional transport. The selectivity of lipids recruited for this vesicular transport could then be a major regulator of local lipid enrichment into submicrometric domains, as discussed for yeast in [169].

5.4. Extrinsic factors

Environmental factors including temperature, solvent properties (*e.g.* pH, osmotic shock) or membrane tension also affect submicrometric domains. Temperature is an essential factor to take into account since each lipid species has its own T*m* (see Section 2.1). The importance of temperature for lipid domains is illustrated by the following observations, *a.o.* In RBCs, the abundance of submicrometric domains enriched in polar lipids or cholesterol (Fig. 7a,d,e) shows a strong dependence on temperature [26, 30, 146]. In activated platelets, submicrometric domains are more abundant at cold than at physiological temperature [91]. In native pulmonary surfactant membranes or in derived human skin stratum corneum

membranes, a slight change of temperature induces a dramatic phase transition [16, 18]. The effect of temperature on domains can be explained by the change into acyl chain conformation beyond the T*m* as discussed in Section 2.1. Besides temperature, pH seems also important for domain formation, as illustrated in derived human skin stratum corneum membranes: pH ~5-6 induces micrometric domains, in contrast to pH 7 which renders lipid organization homogenous and pH 8 which destabilizes lipid membrane architecture [18]. These observations suggest that changes in lipid ionization upon pH modifications affect lipid molecule interactions into submicrometric domains. The perturbation of osmolarity, which is due to a change in ions in the medium and can modulate membrane tension, represents a third factor able to modulate lipid domains. For example, RBC swelling after hypotonic shock induces a reversible coalescence of SM submicrometric domains [30]. Cell stretching can also modulate membrane tension, affecting lipid organization into domains. We have shown this effect using RBCs spread onto poly-L-lysine-coated coverslips, where stretching forces decrease the abundance and size of submicrometric domains [27].

6. Physiopathological significance

Visualization of submicrometric lipid domains raises the question of their physiopathological significance in the life of the cell. Four, not mutually exclusive, roles can be hypothesized, including: (i) membrane reservoir for global cell deformation; (ii) local membrane vesiculation sites; (iii) platforms for protein recruitment and/or activation; and (iv) platforms for subversion by infectious agents (Fig. 8). These different mechanisms might coexist, depending on the type of lipid domain involved and on the morphological, biochemical and functional properties of the cell.

6.1. Membrane reservoir

Analogous to caveolae in endothelial cells [211], submicrometric lipid domains may promote lipid resilience to sustain membrane deformability during cytokinesis, cell polarization or cell squeezing (Fig. 8a). For example, by super-resolution fluorescence microscopy, labeling with fluorescent lysenin and theta fragments and expression of the PH-PLCδ1 domain has revealed that cytokinesis of HeLa cells requires the recruitment of SM, cholesterol and PIP_2 in domains around the cleavage furrow [23]. Similarly, microscopy experiments using Laurdan reveal that organization in ordered domains of the yeast membrane at the mating projection depends on SLs [212]. Lipid domains could also play a role in cell polarization, as exemplified by the concentration of PE at polarized ends in budding yeast [213] and by the main localization of SM-enriched domains at the basolateral membrane of differentiated epithelial cells [114]. Finally, lipid domains could promote cell deformability. All cells are subjected to deformations and this is a critical feature for numerous physiological processes, such as squeezing of RBCs across the narrow pores of the spleen. Other examples include squeezing of cancer cells through tight spaces to invade tissues [214] or formation of the phagocytic cup [215] and the immunological synapse [141]. Regarding RBCs, our group hypothesizes that submicrometric lipid domains could provide stretchable membrane reservoirs when they squeeze into the narrow pores of the spleen, a process occurring >10,000 times during their 120-days lifetime. This hypothesis is currently tested by biophysical approaches.

6.2. Membrane vesiculation sites

In the early 90's, Lipowsky proposed a theoretical model predicting the local budding and vesiculation of the PM when membrane lipid and/or protein domains become unstable at a certain size [190]. This vesiculation process depends on different properties including: (i) the composition of the two membrane leaflets; (ii) the shapes of lipids and proteins present in the bilayer; (iii) the bending energy due to the resultant bilayer rigidity and the line tension on domain edges; (iv) the size of the domains; and (v) the membrane:cytoskeleton anchorage [190, 191]. This theoretical model is supported by the following experimental observations *a.o.*. First, in GUVs, Ld phases tend to spontaneously reside in curved membrane regions whereas Lo phases are preferentially localized in flat regions [216]. This was also shown by molecular dynamics simulations [217]. Second, in living keratinocytes labeled by the Ld marker DiIC18 and the Lo marker CTxB-FITC, submicrometric membrane separation and spontaneous vesiculation of the Ld domains occur. Such vesiculation is still increased upon cholesterol depletion, which further enhances Lo/Ld domain separation and the detachment of the cortical cytoskeleton from the membrane [218]. Third, microvesicles released from activated neutrophils are enriched in cholesterol, which seems essential for microvesicle formation [219]. This observation suggests that lipid rafts or larger lipid domains of particular composition might be the starting point of the vesiculation process. This might explain how microvesicles of the same cellular origin may have different protein and lipid composition [220]. Fourth, it is well-known that senescent RBCs loose membrane by vesiculation (Fig. 7f illustrates this point by labeling of cholesterol with theta toxin fragment; unpublished). Similarly, in spherocytosis, a RBC membrane fragility disease which leads to the release of microvesicles, our unpublished data suggest that SM-enriched domains represent vesiculation sites.

Microvesicles derived from PMs are found in all body fluids and were for a long time considered as inert cellular fragments. However, during the last few years, the hypothesis that microvesicles have crucial roles in both physiological and pathological processes has emerged (see Fig. 8b). Microvesicles are involved in intercellular communication [221, 222], coagulation [223], inflammation [223, 224], tumorigenesis [191], migration [225] and parasitism [226]. Microvesicles are also proposed to play a role during RBC senescence by two opposite mechanisms. They may (i) prevent the elimination of the senescent but yet functional RBCs, by elimination of band3 neoantigen, denatured hemoglobin and oxidized proteins [227]); or instead (ii) promote removal of senescent RBCs from the circulation, by elimination of CD47, a marker of self [228]. In addition to RBC senescence [229], microvesiculation is also observed in blood bags destined to transfusion [230] and is altered in RBC diseases such as spherocytosis, sickle cell disease or thalassemia [231]. Microvesicles might also represent interesting diagnostic biomarkers [232, 233] and even be used in therapeutic applications [234].

6.3. Regulation of protein distribution

As proposed for lipid rafts, domains of particular lipid composition may serve as recruitment or exclusion platforms for membrane proteins, participating in the spatiotemporal regulation of dynamic cellular events (Fig. 8c). A recent study inspired the idea that confinement of proteins facilitates reaction bursts instead of constant and weak reactions [235]. Several

membrane biophysical properties, such as thickness, charge and curvature, could affect protein recruitment or exclusion. These properties depend on the lipid bilayer composition and are thus likely different between lipid domains. Whereas membrane biophysical properties were extensively studied on simple lipid mixtures, the diversity of PM lipid composition of different cells renders the situation more complex. Moreover when proteins are added to the picture, lipids and proteins tend to perturb the properties of each other [236-238]. To minimize energy loss, the hydrophobic thickness of the protein should be equal to the lipid bilayer thickness [236, 239]. Most of the time, the protein tends to localize in a part of the bilayer where the hydrophobic thickness is favorable. If, for some reason, the protein does not find a match, neighboring lipids could adjust to the protein requirements. Proteins can also tilt to hide the hydrophobic part of their transmembrane domain in the hydrophobic part of the bilayer. But if the mismatch is too important, the protein can aggregate to decrease the energy loss [239, 240]. Hydrophobic mismatching may be used to sort proteins in function of the length of their hydrophobic regions to specific compartments and/or membrane domains. Van Galen and coll. recently showed modified organization of functional enzymatic domains and differential sorting of transmembrane proteins in the Trans-Golgi network after disruption of SM homeostasis [241].

The global membrane charge seems to play an additional role in protein sorting. The inner PM leaflet is the most negatively charged membrane of all cell bilayers, attributed to its high PI and PS contents. Through ionic interactions, these acidic phospholipids can favor the targeting of membrane proteins with a polybasic sequence or induce membrane protein clustering to confined regions (see Section 5.2.1). The interaction of polybasic sequences with acidic phospholipids can instead cause steric hindrance and limit the accessibility to other proteins. This process is used during the activation of T cell receptor (TCR) upon antigen engagement. TCR interacts with acidic phospholipids through ionic interactions in quiescent T cells, resulting into deep membrane insertion of the tyrosine side chains. This renders TCR inaccessible to phosphorylation by the Srckinase Lck. After antigen engagement of TCR, local calcium concentration increases, leading to disruption of the ionic protein-lipid interaction, dissociation of tyrosines from the membrane and accessibility to Lck [242, 243].

Finally, membrane curvature, generated by the creation of lipid asymmetry between the two leaflets or by the application of forces or mechanical constraints to the membrane, can also influence protein distribution [244]. For example, the voltage-dependent K^+ channel KvAP is heterogeneously distributed with greater enrichment in highly curved GUV membranes after artificial micropipette bending [245]. The intrinsic shape of a protein may be a critical factor to attribute a place in a certain membrane region in adequacy with the membrane curvature [246].

6.4. Subversion by infectious agents

The PM represents a barrier to external aggression. Therefore, membrane lipids may be targets/receptors of infectious agents such as bacteria and their associated toxins, viruses or parasites. GSLs represent prime targets for toxin and viral binding (Fig. 8d). The paradigm of this behavior is the bacterial cholera toxin that specifically binds to ganglioside GM1 by

its B subunit. After endocytosis of the complex GM1-cholera toxin and transport to the endoplasmic reticulum, the A subunit is unfolded and translocated to the cytosol to induce toxicity [247]. The B subunit has been shown to induce sterol-dependent raft coalescence into submicrometric phases in PM spheres [47]. Shiga toxin, which binds the globotriosylceramide Gb3, induces large lipid domains leading to negative membrane curvature and inward tubulation [248]. Likewise, Simian virus 40 (SV40) binds to ganglioside GM1 and induces similar membrane invagination [249]. The human immunodeficiency virus (HIV) was also shown to colocalize with GM1 and with DiIC16 into domains [250]. SM-enriched domains represent another target for toxins such as lysenin, inducing cytolysis [114]. Cer is also a pertinent candidate in infectious biology for its ability to cluster into gel-like domains, a prerequisite for different infections (for a review, see [251]). In this regard, *Pseudomonas aeruginosa* has been shown to form Cer submicrometric domains in host cells by activation of SMase that hydrolyses SM into Cer [33]. Similarly, *Plasmodium falciparum* activates host as well as pathogen SMases, inducing Cer domains and the generation of a parasitic cavity inside RBCs [252]. These few examples demonstrate that SL submicrometric domains are important in infectious diseases, representing potential targets for treatments.

7. Conclusions & future challenges

In this review, we have highlighted that studying membrane lipid lateral heterogeneity requires a combination of appropriate fluorescent tools, innovative technologies as well as simple and well-characterized cell models. Regarding probes, we have overviewed established probes for the most abundant lipids (Sections 2.2.1 and 3.1; Fig. 3), highlighting their respective advantages and drawbacks. The take-home message is that, whereas several new probes for outer PM leaflet lipids were established and validated during the past decade, such as toxin fragments, only a few are developed for inner PM lipids. Moreover, among available probes, some present limitations, including need of fixation and cytotoxicity. The “ideal” probe would be a small, non-toxic and specific marker of endogenous lipids that can be used on living cells and which exhibits good spectral properties. However, to the best of our knowledge, such probes are not currently available. Therefore, designing of new probes for several lipids would represent a central future challenge. In the meantime, a way to work is to compare several probes for a same target lipid, when available. As an example, double labeling of living RBCs with lysenin toxin fragment, specific to endogenous SM, then with the fluorescent analog BODIPY-SM, reveals the same submicrometric domains (Fig. 6 [26]). Once validated, probes can then be combined to study spatial relation between lipids located in the same PM leaflet, or in one leaflet *vs* another. For instance, electron microscopy of Jurkat T-cells double labeled with lysenin fragment and CTxB shows that SM- and GM1-rich domains are distinct, indicating the dissociation of these two lipids in the outer PM leaflet [24]. In addition, by super-resolution microscopy of LLC-PK1 cells, a superposition of SM clusters in the outer PM leaflet and PIP_2 in the inner leaflet has been shown, indicating a transbilayer colocalization between these two lipids [23]. Thus, combination of validated probes allows to build a map of membrane lipid lateral and transversal organization. Like for probes, even recent technological approaches, such as super-resolution techniques, have their own limitations, as discussed above (Section 3.2; Fig. 4).

Last but not least, it is critical to start with a cell model which is at the same time simple (featureless surface, no lipid turnover nor vesicular trafficking, facilitating data interpretation) and well-characterized (Section 3.3).

Despite known limitations of probes and imaging techniques, morphological evidence for stable submicrometric lipid domains was reported for a variety of cells from prokaryotes to yeast and mammalian cells (Section 4; Table 1). This represents a second revision of the Singer-Nicolson model, after the nanometric lipid rafts concept. As highlighted at Section 6 and summarized at Fig. 8, this new view of membrane organization into submicrometric domains could confer the size and stability required for PMs to (i) deform (*e.g.* during RBC or cancer cell squeezing, cell migration, cytodieresis, cell polarization or formation of the immunological synapse); (ii) locally vesiculate (*e.g.* cell-cell communication, cell migration, tumorigenesis, RBC senescence and membrane fragility diseases); (iii) regulate membrane protein distribution (*e.g.* brain development, SNARE complex, TCR signaling); or (iv) be subverted by infectious agents. Whereas some groups have identified submicrometric lipid domains as targets for protein recruitment (Section 6.3) and for infectious agents (6.4), the two other potential roles remain to be demonstrated.

However, caution should be exercised when generalizing submicrometric lipid domains. We identified several reasons that may help explaining why submicrometric domains have been missed or neglected. In addition to technical issues (spectral properties of tracers, fixation, temperature of examination), global PM lipid composition and membrane:cytoskeleton anchorage might also represent important factors to explain differences between studies. A first limiting factor for the visualization of submicrometric lipid domains is related to the spectral properties of the tracers used. For example, as compared with BODIPY, NBD requires much higher laser power, due to lower quantum yield, thus inevitably causing accelerated photobleaching. Fixation, necessary for some compounds/imaging methods, must be considered as a second limitation since membrane protein long-range movement is even not fully arrested after fixation with formaldehyde and low concentration of glutaraldehyde [253]. This is why some groups favor vital confocal imaging instead of super-resolution microscopy on fixed cells despite lower resolution. Temperature of examination represents a third technical issue. Indeed, domain abundance strongly varies with temperature, a possible cause of non-reproducibility. Besides technical issues, lipid membrane composition, in particular the abundance of cholesterol and SLs, can considerably vary between cell PMs (see Table 3). Finally, unequal membrane:cytoskeleton anchorage, particularly strong in RBCs and myoblasts, could also potentially explain differences in lipid PM distribution among cell types. Likewise, the presence of a cell wall as in yeast should also be considered.

In conclusion, one major challenge that our field faces is to evaluate whether lipid domains can be generalized or if they are restricted to cells exhibiting particular membrane lipid and protein composition, biophysical properties and/or membrane:cytoskeleton anchorage. In addition, various key questions remain poorly understood and are suggested fields for future investigations, including: (i) what is the exact size and diversity of lipid domains?; (ii) to what extent do nanometric rafts undergo regulated coalescence into submicrometric domains under various appropriate conditions, as already suggested for the immunological synapse

[141] and for platelet activation [59, 91]?; (iii) is there a correspondence between lipid domains at outer and inner PM leaflets?; (iv) how can protein:lipid interactions *vs* intrinsic lipid packing be integrated to regulate domains?; and (v) what are the physiopathological roles of domains?.

Acknowledgments

This work was supported by UCL (FSR, DT), the F.R.S-FNRS (DT), the Salus Sanguinis foundation (DT), the Belgian American Educational Foundation, the National Multiple Sclerosis Society (LDA), The Legacy of Angels Foundation (ERB) and the National Institutes of Health (R01 NS065808, ERB). We apologize to all colleagues whose work was not cited due to space constriction. We thank Pierre J. Courtoy (UCL, Belgium) for stimulating scientific discussions.

Abbreviations

AFM	atomic force microscopy
BODIPY	4,4-difluoro-5,7-dimethyl-4-bora-3a,4a-diaza-*s*-indacene
BSA	bovine serum albumin
Cer	ceramide
CTxB	cholera toxin B subunit
DHE	dehydroergosterol
DiI	dialkylindocarbocyanine
DPH	diphenylhexatriene
FRAP	fluorescence recovery after photobleaching
GPMV	giant plasma membrane vesicle
GPI	glycosylphosphatidylinositol
GSL	glycosphingolipid
GUV	giant unilamellar vesicle
LacCer	lactosylceramide
Ld	liquid-disordered
Lo	liquid-ordered
mAb	monoclonal antibody
NBD	7-nitrobenz-2-oxa-1,3-diazol-4-yl
PC	phosphatidylcholine
PE	phosphatidylethanolamine
PH	pleckstrin homology
PI	phosphatidylinositol
PIP_2	phosphatidylinositol-4,5-bisphosphate

PM	plasma membrane
PS	phosphatidylserine
RBC	red blood cell
SIMS	secondary ion mass spectrometry
SL	sphingolipid
SM	sphingomyelin
SMase	sphingomyelinase
So	solid-ordered
TIRF	total internal reflection fluorescence
T*m*	melting temperature

References

1. Takamori S, Holt M, Stenius K, Lemke EA, Gronborg M, Riedel D, et al. Molecular anatomy of a trafficking organelle. Cell. 2006; 127:831–46. [PubMed: 17110340]
2. Gennis, RB. Biomembranes, molecular structure and function. New York: 1989.
3. Ivanova PT, Milne SB, Myers DS, Brown HA. Lipidomics: a mass spectrometry based systems level analysis of cellular lipids. Curr Opin Chem Biol. 2009; 13:526–31. [PubMed: 19744877]
4. van Meer G, Voelker DR, Feigenson GW. Membrane lipids: where they are and how they behave. Nature reviews Molecular cell biology. 2008; 9:112–24. [PubMed: 18216768]
5. Singer SJ, Nicolson GL. The fluid mosaic model of the structure of cell membranes. Science. 1972; 175:720–31. [PubMed: 4333397]
6. van Meer G, Stelzer EH, Wijnaendts-van-Resandt RW, Simons K. Sorting of sphingolipids in epithelial (Madin-Darby canine kidney) cells. The Journal of cell biology. 1987; 105:1623–35. [PubMed: 3667693]
7. Simons K, Ikonen E. Functional rafts in cell membranes. Nature. 1997; 387:569–72. [PubMed: 9177342]
8. Heerklotz H. Triton promotes domain formation in lipid raft mixtures. Biophys J. 2002; 83:2693–701. [PubMed: 12414701]
9. Pike LJ. Rafts defined: a report on the Keystone Symposium on Lipid Rafts and Cell Function. Journal of lipid research. 2006; 47:1597–8. [PubMed: 16645198]
10. Parton RG, Simons K. The multiple faces of caveolae. Nature reviews Molecular cell biology. 2007; 8:185–94. [PubMed: 17318224]
11. Yanez-Mo M, Barreiro O, Gordon-Alonso M, Sala-Valdes M, Sanchez-Madrid F. Tetraspanin-enriched microdomains: a functional unit in cell plasma membranes. Trends Cell Biol. 2009; 19:434–46. [PubMed: 19709882]
12. Parton RG, del Pozo MA. Caveolae as plasma membrane sensors, protectors and organizers. Nature reviews Molecular cell biology. 2013; 14:98–112. [PubMed: 23340574]
13. Zhang XA, Huang C. Tetraspanins and cell membrane tubular structures. Cell Mol Life Sci. 2012; 69:2843–52. [PubMed: 22450717]
14. Hemler ME. Tetraspanin functions and associated microdomains. Nature reviews Molecular cell biology. 2005; 6:801–11. [PubMed: 16314869]
15. Baumgart T, Hammond AT, Sengupta P, Hess ST, Holowka DA, Baird BA, et al. Large-scale fluid/fluid phase separation of proteins and lipids in giant plasma membrane vesicles. Proceedings of the National Academy of Sciences of the United States of America. 2007; 104:3165–70. [PubMed: 17360623]

16. Bernardino de la Serna J, Perez-Gil J, Simonsen AC, Bagatolli LA. Cholesterol rules: direct observation of the coexistence of two fluid phases in native pulmonary surfactant membranes at physiological temperatures. J Biol Chem. 2004; 279:40715–22. [PubMed: 15231828]
17. Kahya N, Scherfeld D, Bacia K, Poolman B, Schwille P. Probing lipid mobility of raft-exhibiting model membranes by fluorescence correlation spectroscopy. J Biol Chem. 2003; 278:28109–15. [PubMed: 12736276]
18. Plasencia I, Norlen L, Bagatolli LA. Direct visualization of lipid domains in human skin stratum corneum's lipid membranes: effect of pH and temperature. Biophys J. 2007; 93:3142–55. [PubMed: 17631535]
19. Yechiel E, Edidin M. Micrometer-scale domains in fibroblast plasma membranes. The Journal of cell biology. 1987; 105:755–60. [PubMed: 3624308]
20. Rodgers W, Glaser M. Characterization of lipid domains in erythrocyte membranes. Proceedings of the National Academy of Sciences of the United States of America. 1991; 88:1364–8. [PubMed: 1996337]
21. Fujiwara T, Ritchie K, Murakoshi H, Jacobson K, Kusumi A. Phospholipids undergo hop diffusion in compartmentalized cell membrane. The Journal of cell biology. 2002; 157:1071–81. [PubMed: 12058021]
22. Mizuno H, Abe M, Dedecker P, Makino A, Rocha S, Ohno-Iwashita Y, et al. Fluorescent probes for superresolution imaging of lipid domains on the plasma membrane. Chem Sci. 2011; 2:1548–53.
23. Abe M, Makino A, Hullin-Matsuda F, Kamijo K, Ohno-Iwashita Y, Hanada K, et al. A role for sphingomyelin-rich lipid domains in the accumulation of phosphatidylinositol-4,5-bisphosphate to the cleavage furrow during cytokinesis. Mol Cell Biol. 2012; 32:1396–407. [PubMed: 22331463]
24. Kiyokawa E, Baba T, Otsuka N, Makino A, Ohno S, Kobayashi T. Spatial and functional heterogeneity of sphingolipid-rich membrane domains. J Biol Chem. 2005; 280:24072–84. [PubMed: 15840575]
25. Frisz JF, Lou K, Klitzing HA, Hanafin WP, Lizunov V, Wilson RL, et al. Direct chemical evidence for sphingolipid domains in the plasma membranes of fibroblasts. Proceedings of the National Academy of Sciences of the United States of America. 2013; 110:E613–22. [PubMed: 23359681]
26. Carquin M, Pollet H, Veiga-da-Cunha M, Cominelli A, Van Der Smissen P, N'Kuli F, et al. Endogenous sphingomyelin segregates into submicrometric domains in the living erythrocyte membrane. Journal of lipid research. 2014; 55:1331–42. [PubMed: 24826836]
27. D'Auria L, Fenaux M, Aleksandrowicz P, Van Der Smissen P, Chantrain C, Vermylen C, et al. Micrometric segregation of fluorescent membrane lipids: relevance for endogenous lipids and biogenesis in erythrocytes. Journal of lipid research. 2013; 54:1066–76. [PubMed: 23322884]
28. Sanchez SA, Tricerri MA, Gratton E. Laurdan generalized polarization fluctuations measures membrane packing micro-heterogeneity in vivo. Proceedings of the National Academy of Sciences of the United States of America. 2012; 109:7314–9. [PubMed: 22529342]
29. Carquin M, Conrard L, Pollet H, Van Der Smissen P, Cominelli A, Veiga-da-Cunha M, et al. Cholesterol segregates into submicrometric domains at the living erythrocyte membrane: evidence and regulation. Cell Mol Life Sci. 2015; 72:4633–51. [PubMed: 26077601]
30. Tyteca D, D'Auria L, Van Der Smissen P, Medts T, Carpentier S, Monbaliu JC, et al. Three unrelated sphingomyelin analogs spontaneously cluster into plasma membrane micrometric domains. Biochimica et biophysica acta. 2010; 1798:909–27. [PubMed: 20123084]
31. Bach JN, Bramkamp M. Flotillins functionally organize the bacterial membrane. Mol Microbiol. 2013; 88:1205–17. [PubMed: 23651456]
32. Grossmann G, Opekarova M, Malinsky J, Weig-Meckl I, Tanner W. Membrane potential governs lateral segregation of plasma membrane proteins and lipids in yeast. The EMBO journal. 2007; 26:1–8. [PubMed: 17170709]
33. Grassme H, Jendrossek V, Riehle A, von Kurthy G, Berger J, Schwarz H, et al. Host defense against Pseudomonas aeruginosa requires ceramide-rich membrane rafts. Nat Med. 2003; 9:322–30. [PubMed: 12563314]
34. Stancevic B, Kolesnick R. Ceramide-rich platforms in transmembrane signaling. FEBS Lett. 2010; 584:1728–40. [PubMed: 20178791]

35. Goni FM. The basic structure and dynamics of cell membranes: an update of the Singer-Nicolson model. Biochimica et biophysica acta. 2014; 1838:1467–76. [PubMed: 24440423]
36. Cai M, Zhao W, Shang X, Jiang J, Ji H, Tang Z, et al. Direct evidence of lipid rafts by in situ atomic force microscopy. Small. 2012; 8:1243–50. [PubMed: 22351491]
37. Wilson RL, Frisz JF, Klitzing HA, Zimmerberg J, Weber PK, Kraft ML. Hemagglutinin clusters in the plasma membrane are not enriched with cholesterol and sphingolipids. Biophys J. 2015; 108:1652–9. [PubMed: 25863057]
38. Honigmann A, Mueller V, Ta H, Schoenle A, Sezgin E, Hell SW, et al. Scanning STED-FCS reveals spatiotemporal heterogeneity of lipid interaction in the plasma membrane of living cells. Nature communications. 2014; 5:5412.
39. Sevcsik E, Brameshuber M, Folser M, Weghuber J, Honigmann A, Schutz GJ. GPI-anchored proteins do not reside in ordered domains in the live cell plasma membrane. Nature communications. 2015; 6:6969.
40. Lingwood D, Simons K. Lipid rafts as a membrane-organizing principle. Science. 2010; 327:46–50. [PubMed: 20044567]
41. Fidorra M, Duelund L, Leidy C, Simonsen AC, Bagatolli LA. Absence of fluid-ordered/fluid-disordered phase coexistence in ceramide/POPC mixtures containing cholesterol. Biophys J. 2006; 90:4437–51. [PubMed: 16565051]
42. Dietrich C, Bagatolli LA, Volovyk ZN, Thompson NL, Levi M, Jacobson K, et al. Lipid rafts reconstituted in model membranes. Biophys J. 2001; 80:1417–28. [PubMed: 11222302]
43. Bagatolli LA. To see or not to see: lateral organization of biological membranes and fluorescence microscopy. Biochimica et biophysica acta. 2006; 1758:1541–56. [PubMed: 16854370]
44. Pinto SN, Silva LC, de Almeida RF, Prieto M. Membrane domain formation, interdigitation, and morphological alterations induced by the very long chain asymmetric C24:1 ceramide. Biophys J. 2008; 95:2867–79. [PubMed: 18586849]
45. Haverstick DM, Glaser M. Visualization of Ca2+-induced phospholipid domains. Proceedings of the National Academy of Sciences of the United States of America. 1987; 84:4475–9. [PubMed: 3474616]
46. Levental I, Grzybek M, Simons K. Raft domains of variable properties and compositions in plasma membrane vesicles. Proceedings of the National Academy of Sciences of the United States of America. 2011; 108:11411–6. [PubMed: 21709267]
47. Lingwood D, Ries J, Schwille P, Simons K. Plasma membranes are poised for activation of raft phase coalescence at physiological temperature. Proceedings of the National Academy of Sciences of the United States of America. 2008; 105:10005–10. [PubMed: 18621689]
48. Chiantia S, Schwille P, Klymchenko AS, London E. Asymmetric GUVs prepared by MbetaCD-mediated lipid exchange: an FCS study. Biophys J. 2011; 100:L1–3. [PubMed: 21190650]
49. Sengupta P, Hammond A, Holowka D, Baird B. Structural determinants for partitioning of lipids and proteins between coexisting fluid phases in giant plasma membrane vesicles. Biochimica et biophysica acta. 2008; 1778:20–32. [PubMed: 17936718]
50. Bagatolli LA. Membrane domains and their relevance to the organization of biological membranes. Comprehensive Biophysics. 2012:16–36.
51. Veatch SL, Keller SL. Miscibility phase diagrams of giant vesicles containing sphingomyelin. Phys Rev Lett. 2005; 94:148101. [PubMed: 15904115]
52. Sun M, Northup N, Marga F, Huber T, Byfield FJ, Levitan I, et al. The effect of cellular cholesterol on membrane-cytoskeleton adhesion. Journal of cell science. 2007; 120:2223–31. [PubMed: 17550968]
53. Parton RG, Way M, Zorzi N, Stang E. Caveolin-3 associates with developing T-tubules during muscle differentiation. The Journal of cell biology. 1997; 136:137–54. [PubMed: 9008709]
54. Laurenzana A, Fibbi G, Chilla A, Margheri G, Del Rosso T, Rovida E, et al. Lipid rafts: integrated platforms for vascular organization offering therapeutic opportunities. Cell Mol Life Sci. 2015
55. Baumann P, Thiele W, Cremers N, Muppala S, Krachulec J, Diefenbacher M, et al. CD24 interacts with and promotes the activity of c-src within lipid rafts in breast cancer cells, thereby increasing integrin-dependent adhesion. Cell Mol Life Sci. 2012; 69:435–48. [PubMed: 21710320]

56. Chichili GR, Rodgers W. Cytoskeleton-membrane interactions in membrane raft structure. Cell Mol Life Sci. 2009; 66:2319–28. [PubMed: 19370312]
57. Veiga MP, Arrondo JL, Goni FM, Alonso A, Marsh D. Interaction of cholesterol with sphingomyelin in mixed membranes containing phosphatidylcholine, studied by spin-label ESR and IR spectroscopies. A possible stabilization of gel-phase sphingolipid domains by cholesterol. Biochemistry. 2001; 40:2614–22. [PubMed: 11327885]
58. Fidorra M, Heimburg T, Bagatolli LA. Direct visualization of the lateral structure of porcine brain cerebrosides/POPC mixtures in presence and absence of cholesterol. Biophys J. 2009; 97:142–54. [PubMed: 19580752]
59. Bali R, Savino L, Ramirez DA, Tsvetkova NM, Bagatolli L, Tablin F, et al. Macroscopic domain formation during cooling in the platelet plasma membrane: an issue of low cholesterol content. Biochimica et biophysica acta. 2009; 1788:1229–37. [PubMed: 19341703]
60. Castro BM, Prieto M, Silva LC. Ceramide: a simple sphingolipid with unique biophysical properties. Prog Lipid Res. 2014; 54:53–67. [PubMed: 24513486]
61. Sot J, Bagatolli LA, Goni FM, Alonso A. Detergent-resistant, ceramide-enriched domains in sphingomyelin/ceramide bilayers. Biophys J. 2006; 90:903–14. [PubMed: 16284266]
62. Sezgin E, Levental I, Grzybek M, Schwarzmann G, Mueller V, Honigmann A, et al. Partitioning, diffusion, and ligand binding of raft lipid analogs in model and cellular plasma membranes. Biochimica et biophysica acta. 2012; 1818:1777–84. [PubMed: 22450237]
63. Heilemann M, van de Linde S, Mukherjee A, Sauer M. Super-resolution imaging with small organic fluorophores. Angewandte Chemie. 2009; 48:6903–8. [PubMed: 19670280]
64. van de Linde S, Heilemann M, Sauer M. Live-cell super-resolution imaging with synthetic fluorophores. Annual review of physical chemistry. 2012; 63:519–40.
65. Resch-Genger U, Grabolle M, Cavaliere-Jaricot S, Nitschke R, Nann T. Quantum dots versus organic dyes as fluorescent labels. Nat Methods. 2008; 5:763–75. [PubMed: 18756197]
66. Fernandez-Suarez M, Ting AY. Fluorescent probes for super-resolution imaging in living cells. Nature reviews Molecular cell biology. 2008; 9:929–43. [PubMed: 19002208]
67. Patterson G, Davidson M, Manley S, Lippincott-Schwartz J. Superresolution imaging using single-molecule localization. Annual review of physical chemistry. 2010; 61:345–67.
68. Wang TY, Silvius JR. Different sphingolipids show differential partitioning into sphingolipid/cholesterol-rich domains in lipid bilayers. Biophys J. 2000; 79:1478–89. [PubMed: 10969009]
69. Lipsky NG, Pagano RE. A vital stain for the Golgi apparatus. Science. 1985; 228:745–7. [PubMed: 2581316]
70. Lipsky NG, Pagano RE. Sphingolipid metabolism in cultured fibroblasts: microscopic and biochemical studies employing a fluorescent ceramide analogue. Proceedings of the National Academy of Sciences of the United States of America. 1983; 80:2608–12. [PubMed: 6573674]
71. Martin OC, Comly ME, Blanchette-Mackie EJ, Pentchev PG, Pagano RE. Cholesterol deprivation affects the fluorescence properties of a ceramide analog at the Golgi apparatus of living cells. Proceedings of the National Academy of Sciences of the United States of America. 1993; 90:2661–5. [PubMed: 8464873]
72. Chattopadhyay A. Chemistry and biology of N-(7-nitrobenz-2-oxa-1,3-diazol-4-yl)-labeled lipids: fluorescent probes of biological and model membranes. Chem Phys Lipids. 1990; 53:1–15. [PubMed: 2191793]
73. Johnson ID, Kang HC, Haugland RP. Fluorescent membrane probes incorporating dipyrrometheneboron difluoride fluorophores. Analytical biochemistry. 1991; 198:228–37. [PubMed: 1799206]
74. Kaiser RD, London E. Determination of the depth of BODIPY probes in model membranes by parallax analysis of fluorescence quenching. Biochimica et biophysica acta. 1998; 1375:13–22. [PubMed: 9767081]
75. Wustner D. Fluorescent sterols as tools in membrane biophysics and cell biology. Chem Phys Lipids. 2007; 146:1–25. [PubMed: 17241621]
76. Holtta-Vuori M, Uronen RL, Repakova J, Salonen E, Vattulainen I, Panula P, et al. BODIPY-cholesterol: a new tool to visualize sterol trafficking in living cells and organisms. Traffic. 2008; 9:1839–49. [PubMed: 18647169]

77. Solanko LM, Honigmann A, Midtiby HS, Lund FW, Brewer JR, Dekaris V, et al. Membrane orientation and lateral diffusion of BODIPY-cholesterol as a function of probe structure. Biophys J. 2013; 105:2082–92. [PubMed: 24209853]

78. Shrivastava S, Haldar S, Gimpl G, Chattopadhyay A. Orientation and dynamics of a novel fluorescent cholesterol analogue in membranes of varying phase. The journal of physical chemistry B. 2009; 113:4475–81. [PubMed: 19249840]

79. Wiegand V, Chang TY, Strauss JF 3rd, Fahrenholz F, Gimpl G. Transport of plasma membrane-derived cholesterol and the function of Niemann-Pick C1 Protein. FASEB journal : official publication of the Federation of American Societies for Experimental Biology. 2003; 17:782–4. [PubMed: 12594172]

80. Huang H, McIntosh AL, Atshaves BP, Ohno-Iwashita Y, Kier AB, Schroeder F. Use of dansylcholestanol as a probe of cholesterol behavior in membranes of living cells. Journal of lipid research. 2010; 51:1157–72. [PubMed: 20008119]

81. Sato SB, Ishii K, Makino A, Iwabuchi K, Yamaji-Hasegawa A, Senoh Y, et al. Distribution and transport of cholesterol-rich membrane domains monitored by a membrane-impermeant fluorescent polyethylene glycol-derivatized cholesterol. J Biol Chem. 2004; 279:23790–6. [PubMed: 15026415]

82. Schroeder F, Dempsey ME, Fischer RT. Sterol and squalene carrier protein interactions with fluorescent delta 5,7,9(11)-cholestatrien-3 beta-ol. J Biol Chem. 1985; 260:2904–11. [PubMed: 3972810]

83. Garvik O, Benediktson P, Simonsen AC, Ipsen JH, Wustner D. The fluorescent cholesterol analog dehydroergosterol induces liquid-ordered domains in model membranes. Chem Phys Lipids. 2009; 159:114–8. [PubMed: 19477318]

84. Scheidt HA, Muller P, Herrmann A, Huster D. The potential of fluorescent and spin-labeled steroid analogs to mimic natural cholesterol. J Biol Chem. 2003; 278:45563–9. [PubMed: 12947110]

85. Mukherjee S, Zha X, Tabas I, Maxfield FR. Cholesterol distribution in living cells: fluorescence imaging using dehydroergosterol as a fluorescent cholesterol analog. Biophys J. 1998; 75:1915–25. [PubMed: 9746532]

86. Bagatolli LA, Sanchez SA, Hazlett T, Gratton E. Giant vesicles, Laurdan, and two-photon fluorescence microscopy: evidence of lipid lateral separation in bilayers. Methods Enzymol. 2003; 360:481–500. [PubMed: 12622164]

87. Gaus K, Zech T, Harder T. Visualizing membrane microdomains by Laurdan 2-photon microscopy. Mol Membr Biol. 2006; 23:41–8. [PubMed: 16611579]

88. Lentz BR. Use of fluorescent probes to monitor molecular order and motions within liposome bilayers. Chem Phys Lipids. 1993; 64:99–116. [PubMed: 8242843]

89. Jin L, Millard AC, Wuskell JP, Dong X, Wu D, Clark HA, et al. Characterization and application of a new optical probe for membrane lipid domains. Biophys J. 2006; 90:2563–75. [PubMed: 16415047]

90. Wolkers WF, Crowe LM, Tsvetkova NM, Tablin F, Crowe JH. In situ assessment of erythrocyte membrane properties during cold storage. Mol Membr Biol. 2002; 19:59–65. [PubMed: 11989823]

91. Gousset K, Wolkers WF, Tsvetkova NM, Oliver AE, Field CL, Walker NJ, et al. Evidence for a physiological role for membrane rafts in human platelets. J Cell Physiol. 2002; 190:117–28. [PubMed: 11807818]

92. Sims PJ, Waggoner AS, Wang CH, Hoffman JF. Studies on the mechanism by which cyanine dyes measure membrane potential in red blood cells and phosphatidylcholine vesicles. Biochemistry. 1974; 13:3315–30. [PubMed: 4842277]

93. Spink CH, Yeager MD, Feigenson GW. Partitioning behavior of indocarbocyanine probes between coexisting gel and fluid phases in model membranes. Biochimica et biophysica acta. 1990; 1023:25–33. [PubMed: 2317494]

94. Whitfield GB, Brock TD, Alfred A, David G, E. CH. Filipin, an Antifungal Antibiotic: Isolation and Properties. J Am Chem Soc. 1955; 77:4799–801.

95. Gimpl G, Gehrig-Burger K. Probes for studying cholesterol binding and cell biology. Steroids. 2011; 76:216–31. [PubMed: 21074546]

96. Ziomek CA, Schulman S, Edidin M. Redistribution of membrane proteins in isolated mouse intestinal epithelial cells. The Journal of cell biology. 1980; 86:849–57. [PubMed: 7410482]

97. Stoeckenius W, Schulman JH, Prince LM. The structure of myelin figures and microemulsions as observed with the electron microscope. Kolloid-Zeitschrift. 1960; 169:170–80.

98. Grimmer S, van Deurs B, Sandvig K. Membrane ruffling and macropinocytosis in A431 cells require cholesterol. Journal of cell science. 2002; 115:2953–62. [PubMed: 12082155]

99. Shimada Y, Maruya M, Iwashita S, Ohno-Iwashita Y. The C-terminal domain of perfringolysin O is an essential cholesterol-binding unit targeting to cholesterol-rich microdomains. European journal of biochemistry / FEBS. 2002; 269:6195–203. [PubMed: 12473115]

100. Waheed AA, Shimada Y, Heijnen HF, Nakamura M, Inomata M, Hayashi M, et al. Selective binding of perfringolysin O derivative to cholesterol-rich membrane microdomains (rafts). Proceedings of the National Academy of Sciences of the United States of America. 2001; 98:4926–31. [PubMed: 11309501]

101. Farrand AJ, LaChapelle S, Hotze EM, Johnson AE, Tweten RK. Only two amino acids are essential for cytolytic toxin recognition of cholesterol at the membrane surface. Proceedings of the National Academy of Sciences of the United States of America. 2010; 107:4341–6. [PubMed: 20145114]

102. Nelson LD, Johnson AE, London E. How interaction of perfringolysin O with membranes is controlled by sterol structure, lipid structure, and physiological low pH: insights into the origin of perfringolysin O-lipid raft interaction. J Biol Chem. 2008; 283:4632–42. [PubMed: 18089559]

103. Rossjohn J, Feil SC, McKinstry WJ, Tweten RK, Parker MW. Structure of a cholesterol-binding, thiol-activated cytolysin and a model of its membrane form. Cell. 1997; 89:685–92. [PubMed: 9182756]

104. Iwamoto M, Morita I, Fukuda M, Murota S, Ando S, Ohno-Iwashita Y. A biotinylated perfringolysin O derivative: a new probe for detection of cell surface cholesterol. Biochimica et biophysica acta. 1997; 1327:222–30. [PubMed: 9271264]

105. Ohno-Iwashita Y, Iwamoto M, Ando S, Iwashita S. Effect of lipidic factors on membrane cholesterol topology--mode of binding of theta-toxin to cholesterol in liposomes. Biochimica et biophysica acta. 1992; 1109:81–90. [PubMed: 1504083]

106. Das A, Goldstein JL, Anderson DD, Brown MS, Radhakrishnan A. Use of mutant 125I-perfringolysin O to probe transport and organization of cholesterol in membranes of animal cells. Proceedings of the National Academy of Sciences of the United States of America. 2013; 110:10580–5. [PubMed: 23754385]

107. Ohno-Iwashita Y, Shimada Y, Hayashi M, Iwamoto M, Iwashita S, Inomata M. Cholesterol-binding toxins and anti-cholesterol antibodies as structural probes for cholesterol localization. Sub-cellular biochemistry. 2010; 51:597–621. [PubMed: 20213560]

108. Ishitsuka R, Yamaji-Hasegawa A, Makino A, Hirabayashi Y, Kobayashi T. A lipid-specific toxin reveals heterogeneity of sphingomyelin-containing membranes. Biophys J. 2004; 86:296–307. [PubMed: 14695271]

109. Ishitsuka R, Kobayashi T. Lysenin: a new tool for investigating membrane lipid organization. Anatomical science international. 2004; 79:184–90. [PubMed: 15633456]

110. Abe M, Kobayashi T. Imaging local sphingomyelin-rich domains in the plasma membrane using specific probes and advanced microscopy. Biochimica et biophysica acta. 2013

111. Shogomori H, Kobayashi T. Lysenin: a sphingomyelin specific pore-forming toxin. Biochimica et biophysica acta. 2008; 1780:612–8. [PubMed: 17980968]

112. Kulma M, Herec M, Grudzinski W, Anderluh G, Gruszecki WI, Kwiatkowska K, et al. Sphingomyelin-rich domains are sites of lysenin oligomerization: implications for raft studies. Biochimica et biophysica acta. 2010; 1798:471–81. [PubMed: 20018171]

113. Kwiatkowska K, Hordejuk R, Szymczyk P, Kulma M, Abdel-Shakor AB, Plucienniczak A, et al. Lysenin-His, a sphingomyelin-recognizing toxin, requires tryptophan 20 for cation-selective channel assembly but not for membrane binding. Mol Membr Biol. 2007; 24:121–34. [PubMed: 17453419]

114. Makino A, Abe M, Murate M, Inaba T, Yilmaz N, Hullin-Matsuda F, et al. Visualization of the heterogeneous membrane distribution of sphingomyelin associated with cytokinesis, cell polarity,

and sphingolipidosis. FASEB journal : official publication of the Federation of American Societies for Experimental Biology. 2015; 29:477–93. [PubMed: 25389132]

115. Skocaj M, Bakrac B, Krizaj I, Macek P, Anderluh G, Sepcic K. The sensing of membrane microdomains based on pore-forming toxins. Current medicinal chemistry. 2013; 20:491–501. [PubMed: 23244522]
116. Fishman PH. Role of membrane gangliosides in the binding and action of bacterial toxins. J Membr Biol. 1982; 69:85–97. [PubMed: 6752418]
117. MacKenzie CR, Hirama T, Lee KK, Altman E, Young NM. Quantitative analysis of bacterial toxin affinity and specificity for glycolipid receptors by surface plasmon resonance. J Biol Chem. 1997; 272:5533–8. [PubMed: 9038159]
118. Lauer S, Goldstein B, Nolan RL, Nolan JP. Analysis of cholera toxin-ganglioside interactions by flow cytometry. Biochemistry. 2002; 41:1742–51. [PubMed: 11827518]
119. Hammond AT, Heberle FA, Baumgart T, Holowka D, Baird B, Feigenson GW. Crosslinking a lipid raft component triggers liquid ordered-liquid disordered phase separation in model plasma membranes. Proceedings of the National Academy of Sciences of the United States of America. 2005; 102:6320–5. [PubMed: 15851688]
120. Solovyeva V, Johannes L, Simonsen AC. Shiga toxin induces membrane reorganization and formation of long range lipid order. Soft matter. 2015; 11:186–92. [PubMed: 25376469]
121. McKanna JA, Haigler HT, Cohen S. Hormone receptor topology and dynamics: morphological analysis using ferritin-labeled epidermal growth factor. Proceedings of the National Academy of Sciences of the United States of America. 1979; 76:5689–93. [PubMed: 230489]
122. Harlan JE, Hajduk PJ, Yoon HS, Fesik SW. Pleckstrin homology domains bind to phosphatidylinositol-4,5-bisphosphate. Nature. 1994; 371:168–70. [PubMed: 8072546]
123. Lemmon MA, Ferguson KM. Signal-dependent membrane targeting by pleckstrin homology (PH) domains. Biochem J. 2000; 350(Pt 1):1–18. [PubMed: 10926821]
124. Lemmon MA, Ferguson KM, O'Brien R, Sigler PB, Schlessinger J. Specific and high-affinity binding of inositol phosphates to an isolated pleckstrin homology domain. Proceedings of the National Academy of Sciences of the United States of America. 1995; 92:10472–6. [PubMed: 7479822]
125. Ferguson KM, Lemmon MA, Schlessinger J, Sigler PB. Structure of the high affinity complex of inositol trisphosphate with a phospholipase C pleckstrin homology domain. Cell. 1995; 83:1037–46. [PubMed: 8521504]
126. Fairn GD, Schieber NL, Ariotti N, Murphy S, Kuerschner L, Webb RI, et al. High-resolution mapping reveals topologically distinct cellular pools of phosphatidylserine. The Journal of cell biology. 2011; 194:257–75. [PubMed: 21788369]
127. Yeung T, Gilbert GE, Shi J, Silvius J, Kapus A, Grinstein S. Membrane phosphatidylserine regulates surface charge and protein localization. Science. 2008; 319:210–3. [PubMed: 18187657]
128. Spira F, Mueller NS, Beck G, von Olshausen P, Beig J, Wedlich-Soldner R. Patchwork organization of the yeast plasma membrane into numerous coexisting domains. Nat Cell Biol. 2012; 14:640–8. [PubMed: 22544065]
129. Kay JG, Grinstein S. Sensing phosphatidylserine in cellular membranes. Sensors. 2011; 11:1744–55. [PubMed: 22319379]
130. Lemmon MA. Membrane recognition by phospholipid-binding domains. Nature reviews Molecular cell biology. 2008; 9:99–111. [PubMed: 18216767]
131. Maekawa M, Fairn GD. Molecular probes to visualize the location, organization and dynamics of lipids. Journal of cell science. 2014; 127:4801–12. [PubMed: 25179600]
132. Jackman N, Ishii A, Bansal R. Oligodendrocyte development and myelin biogenesis: parsing out the roles of glycosphingolipids. Physiology (Bethesda). 2009; 24:290–7. [PubMed: 19815855]
133. Soares MM, King SW, Thorpe PE. Targeting inside-out phosphatidylserine as a therapeutic strategy for viral diseases. Nat Med. 2008; 14:1357–62. [PubMed: 19029986]
134. Kuge H, Akahori K, Yagyu K, Honke K. Functional compartmentalization of the plasma membrane of neurons by a unique acyl chain composition of phospholipids. J Biol Chem. 2014; 289:26783–93. [PubMed: 25096572]

135. Gomez-Mouton C, Lacalle RA, Mira E, Jimenez-Baranda S, Barber DF, Carrera AC, et al. Dynamic redistribution of raft domains as an organizing platform for signaling during cell chemotaxis. The Journal of cell biology. 2004; 164:759–68. [PubMed: 14981096]

136. Rock P, Allietta M, Young WW Jr. Thompson TE, Tillack TW. Organization of glycosphingolipids in phosphatidylcholine bilayers: use of antibody molecules and Fab fragments as morphologic markers. Biochemistry. 1990; 29:8484–90. [PubMed: 2252906]

137. Fitzner D, Schneider A, Kippert A, Mobius W, Willig KI, Hell SW, et al. Myelin basic protein-dependent plasma membrane reorganization in the formation of myelin. The EMBO journal. 2006; 25:5037–48. [PubMed: 17036049]

138. Muyldermans S. Nanobodies: natural single-domain antibodies. Annu Rev Biochem. 2013; 82:775–97. [PubMed: 23495938]

139. Hofman EG, Ruonala MO, Bader AN, van den Heuvel D, Voortman J, Roovers RC, et al. EGF induces coalescence of different lipid rafts. Journal of cell science. 2008; 121:2519–28. [PubMed: 18628305]

140. Gomez-Mouton C, Abad JL, Mira E, Lacalle RA, Gallardo E, Jimenez-Baranda S, et al. Segregation of leading-edge and uropod components into specific lipid rafts during T cell polarization. Proceedings of the National Academy of Sciences of the United States of America. 2001; 98:9642–7. [PubMed: 11493690]

141. Tavano R, Gri G, Molon B, Marinari B, Rudd CE, Tuosto L, et al. CD28 and lipid rafts coordinate recruitment of Lck to the immunological synapse of human T lymphocytes. J Immunol. 2004; 173:5392–7. [PubMed: 15494485]

142. Vasanji A, Ghosh PK, Graham LM, Eppell SJ, Fox PL. Polarization of plasma membrane microviscosity during endothelial cell migration. Dev Cell. 2004; 6:29–41. [PubMed: 14723845]

143. McIntosh AL, Gallegos AM, Atshaves BP, Storey SM, Kannoju D, Schroeder F. Fluorescence and multiphoton imaging resolve unique structural forms of sterol in membranes of living cells. J Biol Chem. 2003; 278:6384–403. [PubMed: 12456684]

144. Weber G, Farris FJ. Synthesis and spectral properties of a hydrophobic fluorescent probe: 6-propionyl-2-(dimethylamino)naphthalene. Biochemistry. 1979; 18:3075–8. [PubMed: 465454]

145. Asanov A, Zepeda A, Vaca L. A novel form of Total Internal Reflection Fluorescence Microscopy (LG-TIRFM) reveals different and independent lipid raft domains in living cells. Biochimica et biophysica acta. 2010; 1801:147–55. [PubMed: 19840867]

146. D'Auria L, Van der Smissen P, Bruyneel F, Courtoy PJ, Tyteca D. Segregation of fluorescent membrane lipids into distinct micrometric domains: evidence for phase compartmentation of natural lipids? PloS one. 2011; 6:e17021. [PubMed: 21386970]

147. Golfetto O, Hinde E, Gratton E. Laurdan fluorescence lifetime discriminates cholesterol content from changes in fluidity in living cell membranes. Biophys J. 2013; 104:1238–47. [PubMed: 23528083]

148. Tokumasu F, Crivat G, Ackerman H, Hwang J, Wellems TE. Inward cholesterol gradient of the membrane system in P. falciparum-infected erythrocytes involves a dilution effect from parasite-produced lipids. Biol Open. 2014; 3:529–41. [PubMed: 24876390]

149. Bag N, Yap DH, Wohland T. Temperature dependence of diffusion in model and live cell membranes characterized by imaging fluorescence correlation spectroscopy. Biochimica et biophysica acta. 2014; 1838:802–13. [PubMed: 24600711]

150. Winckler P, Cailler A, Deturche R, Jeannesson P, Morjani H, Jaffiol R. Microfluidity mapping using fluorescence correlation spectroscopy: a new way to investigate plasma membrane microorganization of living cells. Biochimica et biophysica acta. 2012; 1818:2477–85. [PubMed: 22640696]

151. Frisz JF, Klitzing HA, Lou K, Hutcheon ID, Weber PK, Zimmerberg J, et al. Sphingolipid domains in the plasma membranes of fibroblasts are not enriched with cholesterol. J Biol Chem. 2013; 288:16855–61. [PubMed: 23609440]

152. Milhiet PE, Giocondi MC, Le Grimellec C. Cholesterol is not crucial for the existence of microdomains in kidney brush-border membrane models. J Biol Chem. 2002; 277:875–8. [PubMed: 11717303]

153. Orsini F, Cremona A, Arosio P, Corsetto PA, Montorfano G, Lascialfari A, et al. Atomic force microscopy imaging of lipid rafts of human breast cancer cells. Biochimica et biophysica acta. 2012; 1818:2943–9. [PubMed: 22884468]

154. Dufrene YF, Martinez-Martin D, Medalsy I, Alsteens D, Muller DJ. Multiparametric imaging of biological systems by force-distance curve-based AFM. Nat Methods. 2013; 10:847–54. [PubMed: 23985731]

155. Dickenson NE, Armendariz KP, Huckabay HA, Livanec PW, Dunn RC. Near-field scanning optical microscopy: a tool for nanometric exploration of biological membranes. Anal Bioanal Chem. 2010; 396:31–43. [PubMed: 19730836]

156. Chen Y, Qin J, Chen ZW. Fluorescence-topographic NSOM directly visualizes peak-valley polarities of GM1/GM3 rafts in cell membrane fluctuations. Journal of lipid research. 2008; 49:2268–75. [PubMed: 18603643]

157. Deleu M, Crowet JM, Nasir MN, Lins L. Complementary biophysical tools to investigate lipid specificity in the interaction between bioactive molecules and the plasma membrane: A review. Biochimica et biophysica acta. 2014; 1838:3171–90. [PubMed: 25175476]

158. Scherrer R, Louden L, Gerhardt P. Porosity of the yeast cell wall and membrane. Journal of bacteriology. 1974; 118:534–40. [PubMed: 4597447]

159. Zachowski A. Phospholipids in animal eukaryotic membranes: transverse asymmetry and movement. Biochem J. 1993; 294(Pt 1):1–14. [PubMed: 8363559]

160. Goodman SR, Daescu O, Kakhniashvili DG, Zivanic M. The proteomics and interactomics of human erythrocytes. Exp Biol Med (Maywood). 2013; 238:509–18. [PubMed: 23856902]

161. Bramkamp M, Lopez D. Exploring the existence of lipid rafts in bacteria. Microbiology and molecular biology reviews : MMBR. 2015; 79:81–100. [PubMed: 25652542]

162. Donovan C, Bramkamp M. Characterization and subcellular localization of a bacterial flotillin homologue. Microbiology. 2009; 155:1786–99. [PubMed: 19383680]

163. Doughty DM, Dieterle M, Sessions AL, Fischer WW, Newman DK. Probing the subcellular localization of hopanoid lipids in bacteria using NanoSIMS. PloS one. 2014; 9:e84455. [PubMed: 24409299]

164. Mileykovskaya E, Dowhan W. Visualization of phospholipid domains in Escherichia coli by using the cardiolipin-specific fluorescent dye 10-N-nonyl acridine orange. Journal of bacteriology. 2000; 182:1172–5. [PubMed: 10648548]

165. Kawai F, Shoda M, Harashima R, Sadaie Y, Hara H, Matsumoto K. Cardiolipin domains in Bacillus subtilis marburg membranes. Journal of bacteriology. 2004; 186:1475–83. [PubMed: 14973018]

166. Kabeche R, Madrid M, Cansado J, Moseley JB. Eisosomes Regulate Phosphatidylinositol 4,5-Bisphosphate (PI(4,5)P2) Cortical Clusters and Mitogen-activated Protein (MAP) Kinase Signaling upon Osmotic Stress. J Biol Chem. 2015; 290:25960–73. [PubMed: 26359496]

167. Guiney EL, Goldman AR, Elias JE, Cyert MS. Calcineurin regulates the yeast synaptojanin Inp53/Sjl3 during membrane stress. Mol Biol Cell. 2015; 26:769–85. [PubMed: 25518934]

168. Mueller NS, Wedlich-Soldner R, Spira F. From mosaic to patchwork: matching lipids and proteins in membrane organization. Mol Membr Biol. 2012; 29:186–96. [PubMed: 22594654]

169. Schuberth C, Wedlich-Soldner R. Building a patchwork - The yeast plasma membrane as model to study lateral domain formation. Biochimica et biophysica acta. 2015; 1853:767–74. [PubMed: 25541280]

170. Vecer J, Vesela P, Malinsky J, Herman P. Sphingolipid levels crucially modulate lateral microdomain organization of plasma membrane in living yeast. FEBS Lett. 2014; 588:443–9. [PubMed: 24333335]

171. Aresta-Branco F, Cordeiro AM, Marinho HS, Cyrne L, Antunes F, de Almeida RF. Gel domains in the plasma membrane of Saccharomyces cerevisiae: highly ordered, ergosterol-free, and sphingolipid-enriched lipid rafts. J Biol Chem. 2011; 286:5043–54. [PubMed: 21127065]

172. Montes LR, Lopez DJ, Sot J, Bagatolli LA, Stonehouse MJ, Vasil ML, et al. Ceramide-enriched membrane domains in red blood cells and the mechanism of sphingomyelinase-induced hot-cold hemolysis. Biochemistry. 2008; 47:11222–30. [PubMed: 18826261]

173. Hao M, Mukherjee S, Maxfield FR. Cholesterol depletion induces large scale domain segregation in living cell membranes. Proceedings of the National Academy of Sciences of the United States of America. 2001; 98:13072–7. [PubMed: 11698680]
174. Aggarwal S, Yurlova L, Simons M. Central nervous system myelin: structure, synthesis and assembly. Trends Cell Biol. 2011; 21:585–93. [PubMed: 21763137]
175. Nawaz S, Kippert A, Saab AS, Werner HB, Lang T, Nave KA, et al. Phosphatidylinositol 4,5-bisphosphate-dependent interaction of myelin basic protein with the plasma membrane in oligodendroglial cells and its rapid perturbation by elevated calcium. J Neurosci. 2009; 29:4794–807. [PubMed: 19369548]
176. Boggs JM, Wang H. Co-clustering of galactosylceramide and membrane proteins in oligodendrocyte membranes on interaction with polyvalent carbohydrate and prevention by an intact cytoskeleton. Journal of neuroscience research. 2004; 76:342–55. [PubMed: 15079863]
177. Boggs JM, Gao W, Zhao J, Park HJ, Liu Y, Basu A. Participation of galactosylceramide and sulfatide in glycosynapses between oligodendrocyte or myelin membranes. FEBS Lett. 2010; 584:1771–8. [PubMed: 19941861]
178. Ozgen H, Schrimpf W, Hendrix J, de Jonge JC, Lamb DC, Hoekstra D, et al. The lateral membrane organization and dynamics of myelin proteins PLP and MBP are dictated by distinct galactolipids and the extracellular matrix. PloS one. 2014; 9:e101834. [PubMed: 25003183]
179. Decker L, ffrench-Constant C. Lipid rafts and integrin activation regulate oligodendrocyte survival. J Neurosci. 2004; 24:3816–25. [PubMed: 15084663]
180. Baron W, Bijlard M, Nomden A, de Jonge JC, Teunissen CE, Hoekstra D. Sulfatide-mediated control of extracellular matrix-dependent oligodendrocyte maturation. Glia. 2014; 62:927–42. [PubMed: 24578319]
181. Bagatolli LA, Ipsen JH, Simonsen AC, Mouritsen OG. An outlook on organization of lipids in membranes: searching for a realistic connection with the organization of biological membranes. Prog Lipid Res. 2010; 49:378–89. [PubMed: 20478336]
182. Bagatolli LA. Microscopy imaging of membrane domains. Biochimica et biophysica acta. 2010; 1798:1285. [PubMed: 20529670]
183. Goni FM, Alonso A. Effects of ceramide and other simple sphingolipids on membrane lateral structure. Biochimica et biophysica acta. 2009; 1788:169–77. [PubMed: 18848519]
184. Westerlund B, Slotte JP. How the molecular features of glycosphingolipids affect domain formation in fluid membranes. Biochimica et biophysica acta. 2009; 1788:194–201. [PubMed: 19073136]
185. Stott BM, Vu MP, McLemore CO, Lund MS, Gibbons E, Brueseke TJ, et al. Use of fluorescence to determine the effects of cholesterol on lipid behavior in sphingomyelin liposomes and erythrocyte membranes. Journal of lipid research. 2008; 49:1202–15. [PubMed: 18299615]
186. London E. Insights into lipid raft structure and formation from experiments in model membranes. Curr Opin Struct Biol. 2002; 12:480–6. [PubMed: 12163071]
187. Iwabuchi K, Nakayama H, Iwahara C, Takamori K. Significance of glycosphingolipid fatty acid chain length on membrane microdomain-mediated signal transduction. FEBS Lett. 2010; 584:1642–52. [PubMed: 19852959]
188. Singh RD, Liu Y, Wheatley CL, Holicky EL, Makino A, Marks DL, et al. Caveolar endocytosis and microdomain association of a glycosphingolipid analog is dependent on its sphingosine stereochemistry. J Biol Chem. 2006; 281:30660–8. [PubMed: 16893900]
189. Murate M, Kobayashi T. Revisiting transbilayer distribution of lipids in the plasma membrane. Chem Phys Lipids. 2015
190. Lipowsky R. Domain-induced budding of fluid membranes. Biophys J. 1993; 64:1133–8. [PubMed: 19431884]
191. Muralidharan-Chari V, Clancy JW, Sedgwick A, D'Souza-Schorey C. Microvesicles: mediators of extracellular communication during cancer progression. Journal of cell science. 2010; 123:1603–11. [PubMed: 20445011]
192. Lee AG. Biological membranes: The importance of molecular detail. Trends in Biochemical Sciences. 2011; 36:493–500. [PubMed: 21855348]

193. Lee AG, Dalton KA, Duggleby RC, East JM, Starling AP. Lipid structure and Ca(2+)-ATPase function. Biosci Rep. 1995; 15:289–98. [PubMed: 8825031]

194. Shinzawa-Itoh K, Aoyama H, Muramoto K, Terada H, Kurauchi T, Tadehara Y, et al. Structures and physiological roles of 13 integral lipids of bovine heart cytochrome c oxidase. The EMBO journal. 2007; 26:1713–25. [PubMed: 17332748]

195. Contreras FX, Ernst AM, Haberkant P, Bjorkholm P, Lindahl E, Gonen B, et al. Molecular recognition of a single sphingolipid species by a protein's transmembrane domain. Nature. 2012; 481:525–9. [PubMed: 22230960]

196. Janmey PA, Lindberg U. Cytoskeletal regulation: Rich in lipids. Nature Reviews Molecular Cell Biology. 2004; 5:658–66. [PubMed: 15366709]

197. Baines AJ. The spectrin-ankyrin-4.1-adducin membrane skeleton: Adapting eukaryotic cells to the demands of animal life. Protoplasma. 2010; 244:99–131. [PubMed: 20668894]

198. Van Den Bogaart G, Meyenberg K, Risselada HJ, Amin H, Willig KI, Hubrich BE, et al. Membrane protein sequestering by ionic protein-lipid interactions. Nature. 2011; 479:552–5. [PubMed: 22020284]

199. McLaughlin S, Murray D. Plasma membrane phosphoinositide organization by protein electrostatics. Nature. 2005; 438:605–11. [PubMed: 16319880]

200. Levental I, Grzybek M, Simons K. Greasing their way: lipid modifications determine protein association with membrane rafts. Biochemistry. 2010; 49:6305–16. [PubMed: 20583817]

201. Zacharias DA, Violin JD, Newton AC, Tsien RY. Partitioning of lipid-modified monomeric GFPs into membrane microdomains of live cells. Science. 2002; 296:913–6. [PubMed: 11988576]

202. Sharom FJ, Lehto MT. Glycosylphosphatidylinositol-anchored proteins: structure, function, and cleavage by phosphatidylinositol-specific phospholipase C. Biochemistry and cell biology = Biochimie et biologie cellulaire. 2002; 80:535–49. [PubMed: 12440695]

203. Martin DD, Beauchamp E, Berthiaume LG. Post-translational myristoylation: Fat matters in cellular life and death. Biochimie. 2011; 93:18–31. [PubMed: 21056615]

204. Nadolski MJ, Linder ME. Protein lipidation. The FEBS journal. 2007; 274:5202–10. [PubMed: 17892486]

205. Kusumi A, Fujiwara TK, Chadda R, Xie M, Tsunoyama TA, Kalay Z, et al. Dynamic Organizing Principles of the Plasma Membrane that Regulate Signal Transduction: Commemorating the Fortieth Anniversary of Singer and Nicolson's Fluid-Mosaic Model. Annu Rev Cell Dev Biol. 2012; 28:215–50. [PubMed: 22905956]

206. Kusumi A, Fujiwara TK, Morone N, Yoshida KJ, Chadda R, Xie M, et al. Membrane mechanisms for signal transduction: the coupling of the meso-scale raft domains to membrane-skeleton-induced compartments and dynamic protein complexes. Seminars in cell & developmental biology. 2012; 23:126–44. [PubMed: 22309841]

207. Kusumi A, Suzuki KG, Kasai RS, Ritchie K, Fujiwara TK. Hierarchical mesoscale domain organization of the plasma membrane. Trends in biochemical sciences. 2011; 36:604–15. [PubMed: 21917465]

208. Raghupathy R, Anilkumar AA, Polley A, Singh PP, Yadav M, Johnson C, et al. Transbilayer lipid interactions mediate nanoclustering of lipid-anchored proteins. Cell. 2015; 161:581–94. [PubMed: 25910209]

209. Sheetz MP, Sable JE, Dobereiner HG. Continuous membrane-cytoskeleton adhesion requires continuous accommodation to lipid and cytoskeleton dynamics. Annual review of biophysics and biomolecular structure. 2006; 35:417–34.

210. Young ME, Karpova TS, Brugger B, Moschenross DM, Wang GK, Schneiter R, et al. The Sur7p family defines novel cortical domains in Saccharomyces cerevisiae, affects sphingolipid metabolism, and is involved in sporulation. Mol Cell Biol. 2002; 22:927–34. [PubMed: 11784867]

211. Sinha B, Koster D, Ruez R, Gonnord P, Bastiani M, Abankwa D, et al. Cells respond to mechanical stress by rapid disassembly of caveolae. Cell. 2011; 144:402–13. [PubMed: 21295700]

212. Proszynski TJ, Klemm R, Bagnat M, Gaus K, Simons K. Plasma membrane polarization during mating in yeast cells. The Journal of cell biology. 2006; 173:861–6. [PubMed: 16769822]

213. Iwamoto K, Kobayashi S, Fukuda R, Umeda M, Kobayashi T, Ohta A. Local exposure of phosphatidylethanolamine on the yeast plasma membrane is implicated in cell polarity. Genes Cells. 2004; 9:891–903. [PubMed: 15461661]

214. Byun S, Son S, Amodei D, Cermak N, Shaw J, Kang JH, et al. Characterizing deformability and surface friction of cancer cells. Proceedings of the National Academy of Sciences of the United States of America. 2013; 110:7580–5. [PubMed: 23610435]

215. Irmscher M, de Jong AM, Kress H, Prins MW. A method for time-resolved measurements of the mechanics of phagocytic cups. Journal of the Royal Society, Interface / the Royal Society. 2013; 10:20121048.

216. Baumgart T, Hess ST, Webb WW. Imaging coexisting fluid domains in biomembrane models coupling curvature and line tension. Nature. 2003; 425:821–4. [PubMed: 14574408]

217. Wu QY, Liang Q. Interplay between curvature and lateral organization of lipids and peptides/proteins in model membranes. Langmuir. 2014; 30:1116–22. [PubMed: 24417311]

218. Vind-Kezunovic D, Nielsen CH, Wojewodzka U, Gniadecki R. Line tension at lipid phase boundaries regulates formation of membrane vesicles in living cells. Biochimica et biophysica acta. 2008; 1778:2480–6. [PubMed: 18586000]

219. Del Conde I, Shrimpton CN, Thiagarajan P, Lopez JA. Tissue-factor-bearing microvesicles arise from lipid rafts and fuse with activated platelets to initiate coagulation. Blood. 2005; 106:1604–11. [PubMed: 15741221]

220. Hugel B, Martinez MC, Kunzelmann C, Freyssinet JM. Membrane microparticles: two sides of the coin. Physiology (Bethesda). 2005; 20:22–7. [PubMed: 15653836]

221. Mause SF, Weber C. Microparticles: protagonists of a novel communication network for intercellular information exchange. Circulation research. 2010; 107:1047–57. [PubMed: 21030722]

222. Turturici G, Tinnirello R, Sconzo G, Geraci F. Extracellular membrane vesicles as a mechanism of cell-to-cell communication: advantages and disadvantages. American journal of physiology Cell physiology. 2014; 306:C621–33. [PubMed: 24452373]

223. Yuana Y, Sturk A, Nieuwland R. Extracellular vesicles in physiological and pathological conditions. Blood reviews. 2013; 27:31–9. [PubMed: 23261067]

224. Gupta A, Pulliam L. Exosomes as mediators of neuroinflammation. J Neuroinflammation. 2014; 11:68. [PubMed: 24694258]

225. Shen B, Fang Y, Wu N, Gould SJ. Biogenesis of the posterior pole is mediated by the exosome/microvesicle protein-sorting pathway. J Biol Chem. 2011; 286:44162–76. [PubMed: 21865156]

226. Barteneva NS, Maltsev N, Vorobjev IA. Microvesicles and intercellular communication in the context of parasitism. Frontiers in cellular and infection microbiology. 2013; 3:49. [PubMed: 24032108]

227. Willekens FL, Werre JM, Groenen-Dopp YA, Roerdinkholder-Stoelwinder B, de Pauw B, Bosman GJ. Erythrocyte vesiculation: a self-protective mechanism? Br J Haematol. 2008; 141:549–56. [PubMed: 18419623]

228. Stewart A, Urbaniak S, Turner M, Bessos H. The application of a new quantitative assay for the monitoring of integrin-associated protein CD47 on red blood cells during storage and comparison with the expression of CD47 and phosphatidylserine with flow cytometry. Transfusion. 2005; 45:1496–503. [PubMed: 16131383]

229. Bosman GJ, Werre JM, Willekens FL, Novotny VM. Erythrocyte ageing in vivo and in vitro: structural aspects and implications for transfusion. Transfusion medicine (Oxford, England). 2008; 18:335–47.

230. Bosman GJ, Lasonder E, Luten M, Roerdinkholder-Stoelwinder B, Novotny VM, Bos H, et al. The proteome of red cell membranes and vesicles during storage in blood bank conditions. Transfusion. 2008; 48:827–35. [PubMed: 18346024]

231. Gov, N.; Cluitmans, J.; Sens, P.; Bosman, GJCGM.; Liu, AL.; Aleš, I. Advances in Planar Lipid Bilayers and Liposomes. Academic Press; 2009. Chapter 4 Cytoskeletal Control of Red Blood Cell Shape: Theory and Practice of Vesicle Formation.; p. 95-119.

232. Fujita Y, Kuwano K, Ochiya T, Takeshita F. The impact of extracellular vesicle-encapsulated circulating microRNAs in lung cancer research. BioMed research international. 2014; 2014:486413. [PubMed: 25295261]

233. Wang Y, Chen LM, Liu ML. Microvesicles and diabetic complications--novel mediators, potential biomarkers and therapeutic targets. Acta pharmacologica Sinica. 2014; 35:433–43. [PubMed: 24608676]

234. Thoene J, Goss T, Witcher M, Mullet J, N'Kuli F, Van Der Smissen P, et al. In vitro correction of disorders of lysosomal transport by microvesicles derived from baculovirus-infected Spodoptera cells. Molecular genetics and metabolism. 2013; 109:77–85. [PubMed: 23465695]

235. Kalay Z, Fujiwara TK, Kusumi A. Confining domains lead to reaction bursts: reaction kinetics in the plasma membrane. PloS one. 2012; 7:e32948. [PubMed: 22479350]

236. Andersen OS, Koeppe Ii RE. Bilayer thickness and membrane protein function: An energetic perspective. Annual review of biophysics and biomolecular structure. 2007:107–30.

237. Jensen MØ, Mouritsen OG. Lipids do influence protein function - The hydrophobic matching hypothesis revisited. Biochimica et Biophysica Acta - Biomembranes. 2004; 1666:205–26.

238. Phillips R, Ursell T, Wiggins P, Sens P. Emerging roles for lipids in shaping membrane-protein function. Nature. 2009; 459:379–85. [PubMed: 19458714]

239. Killian JA. Hydrophobic mismatch between proteins and lipids in membranes. Biochimica et Biophysica Acta - Reviews on Biomembranes. 1998; 1376:401–15.

240. Lee AG. How lipids affect the activities of integral membrane proteins. Biochimica et Biophysica Acta - Biomembranes. 2004; 1666:62–87.

241. van Galen J, Campelo F, Martinez-Alonso E, Scarpa M, Martinez-Menarguez JA, Malhotra V. Sphingomyelin homeostasis is required to form functional enzymatic domains at the trans-Golgi network. The Journal of cell biology. 2014; 206:609–18. [PubMed: 25179630]

242. Shi X, Bi Y, Yang W, Guo X, Jiang Y, Wan C, et al. Ca2+ regulates T-cell receptor activation by modulating the charge property of lipids. Nature. 2013; 493:111–5. [PubMed: 23201688]

243. Li L, Shi X, Guo X, Li H, Xu C. Ionic protein-lipid interaction at the plasma membrane: what can the charge do? Trends in biochemical sciences. 2014; 39:130–40. [PubMed: 24534649]

244. Graham TR, Kozlov MM. Interplay of proteins and lipids in generating membrane curvature. Curr Opin Cell Biol. 2010; 22:430–6. [PubMed: 20605711]

245. Aimon S, Callan-Jones A, Berthaud A, Pinot M, Toombes GE, Bassereau P. Membrane shape modulates transmembrane protein distribution. Dev Cell. 2014; 28:212–8. [PubMed: 24480645]

246. McMahon HT, Boucrot E. Membrane curvature at a glance. Journal of cell science. 2015; 128:1065–70. [PubMed: 25774051]

247. Chinnapen DJ, Hsieh WT, te Welscher YM, Saslowsky DE, Kaoutzani L, Brandsma E, et al. Lipid sorting by ceramide structure from plasma membrane to ER for the cholera toxin receptor ganglioside GM1. Dev Cell. 2012; 23:573–86. [PubMed: 22975326]

248. Romer W, Berland L, Chambon V, Gaus K, Windschiegl B, Tenza D, et al. Shiga toxin induces tubular membrane invaginations for its uptake into cells. Nature. 2007; 450:670–5. [PubMed: 18046403]

249. Ewers H, Romer W, Smith AE, Bacia K, Dmitrieff S, Chai W, et al. GM1 structure determines SV40-induced membrane invagination and infection. Nat Cell Biol. 2010; 12:11–8. sup pp 1-2. [PubMed: 20023649]

250. Nguyen DH, Hildreth JE. Evidence for budding of human immunodeficiency virus type 1 selectively from glycolipid-enriched membrane lipid rafts. J Virol. 2000; 74:3264–72. [PubMed: 10708443]

251. Gulbins, E.; Petrache, I. Wien. Springer; New York: 2013. Sphingolipids in disease..

252. Gruring C, Heiber A, Kruse F, Ungefehr J, Gilberger TW, Spielmann T. Development and host cell modifications of Plasmodium falciparum blood stages in four dimensions. Nature communications. 2011; 2:165.

253. Tanaka KA, Suzuki KG, Shirai YM, Shibutani ST, Miyahara MS, Tsuboi H, et al. Membrane molecules mobile even after chemical fixation. Nat Methods. 2010; 7:865–6. [PubMed: 20881966]

254. Pristera A, Baker MD, Okuse K. Association between tetrodotoxin resistant channels and lipid rafts regulates sensory neuron excitability. PloS one. 2012; 7:e40079. [PubMed: 22870192]
255. Schutz GJ, Kada G, Pastushenko VP, Schindler H. Properties of lipid microdomains in a muscle cell membrane visualized by single molecule microscopy. The EMBO journal. 2000; 19:892–901. [PubMed: 10698931]
256. Heiner AL, Gibbons E, Fairbourn JL, Gonzalez LJ, McLemore CO, Brueseke TJ, et al. Effects of cholesterol on physical properties of human erythrocyte membranes: impact on susceptibility to hydrolysis by secretory phospholipase A2. Biophys J. 2008; 94:3084–93. [PubMed: 18192373]
257. Vest R, Wallis R, Jensen LB, Haws AC, Callister J, Brimhall B, et al. Use of steady-state laurdan fluorescence to detect changes in liquid ordered phases in human erythrocyte membranes. J Membr Biol. 2006; 211:15–25. [PubMed: 16988865]
258. Parasassi T, Gratton E, Yu WM, Wilson P, Levi M. Two-photon fluorescence microscopy of laurdan generalized polarization domains in model and natural membranes. Biophys J. 1997; 72:2413–29. [PubMed: 9168019]
259. Owen DM, Rentero C, Magenau A, Abu-Siniyeh A, Gaus K. Quantitative imaging of membrane lipid order in cells and organisms. Nat Protoc. 2012; 7:24–35. [PubMed: 22157973]
260. Gaus K, Gratton E, Kable EP, Jones AS, Gelissen I, Kritharides L, et al. Visualizing lipid structure and raft domains in living cells with two-photon microscopy. Proceedings of the National Academy of Sciences of the United States of America. 2003; 100:15554–9. [PubMed: 14673117]
261. Sanderson MJ, Smith I, Parker I, Bootman MD. Fluorescence microscopy. Cold Spring Harb Protoc. 2014; 2014 pdb top071795.
262. Poulter NS, Pitkeathly WT, Smith PJ, Rappoport JZ. The physical basis of total internal reflection fluorescence (TIRF) microscopy and its cellular applications. Methods Mol Biol. 2015; 1251:1–23. [PubMed: 25391791]
263. Sezgin E, Schwille P. Fluorescence techniques to study lipid dynamics. Cold Spring Harb Perspect Biol. 2011; 3:a009803. [PubMed: 21669985]
264. Stockl MT, Herrmann A. Detection of lipid domains in model and cell membranes by fluorescence lifetime imaging microscopy. Biochimica et biophysica acta. 2010; 1798:1444–56. [PubMed: 20056106]
265. Bacia K, Haustein E, Schwille P. Fluorescence correlation spectroscopy: principles and applications. Cold Spring Harb Protoc. 2014; 2014:709–25. [PubMed: 24987147]
266. Nelson AJ, Hess ST. Localization microscopy: mapping cellular dynamics with single molecules. J Microsc. 2014; 254:1–8. [PubMed: 24611627]
267. Schermelleh L, Heintzmann R, Leonhardt H. A guide to super-resolution fluorescence microscopy. The Journal of cell biology. 2010; 190:165–75. [PubMed: 20643879]
268. Xia T, Li N, Fang X. Single-molecule fluorescence imaging in living cells. Annual review of physical chemistry. 2013; 64:459–80.
269. Kraft ML, Klitzing HA. Imaging lipids with secondary ion mass spectrometry. Biochimica et biophysica acta. 2014; 1841:1108–19. [PubMed: 24657337]
270. Epand RM, Epand RF. Bacterial membrane lipids in the action of antimicrobial agents. Journal of peptide science : an official publication of the European Peptide Society. 2011; 17:298–305. [PubMed: 21480436]
271. Dickson RC, Nagiec EE, Wells GB, Nagiec MM, Lester RL. Synthesis of mannose-(inositol-P)2-ceramide, the major sphingolipid in Saccharomyces cerevisiae, requires the IPT1 (YDR072c) gene. J Biol Chem. 1997; 272:29620–5. [PubMed: 9368028]
272. Daum G, Tuller G, Nemec T, Hrastnik C, Balliano G, Cattel L, et al. Systematic analysis of yeast strains with possible defects in lipid metabolism. Yeast. 1999; 15:601–14. [PubMed: 10341423]
273. Biro E, Akkerman JW, Hoek FJ, Gorter G, Pronk LM, Sturk A, et al. The phospholipid composition and cholesterol content of platelet-derived microparticles: a comparison with platelet membrane fractions. Journal of thrombosis and haemostasis : JTH. 2005; 3:2754–63. [PubMed: 16359513]

274. Fauvel J, Chap H, Roques V, Levy-Toledano S, Douste-Blazy L. Biochemical characterization of plasma membranes and intracellular membranes isolated from human platelets using Percoll gradients. Biochimica et biophysica acta. 1986; 856:155–64. [PubMed: 2937454]

275. Pankov R, Markovska T, Antonov P, Ivanova L, Momchilova A. The plasma membrane lipid composition affects fusion between cells and model membranes. Chemico-biological interactions. 2006; 164:167–73. [PubMed: 17098217]

276. Cezanne L, Navarro L, Tocanne JF. Isolation of the plasma membrane and organelles from Chinese hamster ovary cells. Biochimica et biophysica acta. 1992; 1112:205–14. [PubMed: 1457453]

277. Calderon RO, DeVries GH. Lipid composition and phospholipid asymmetry of membranes from a Schwann cell line. Journal of neuroscience research. 1997; 49:372–80. [PubMed: 9260748]

278. Perkins RG, Scott RE. Plasma membrane phospholipid, cholesterol and fatty acyl composition of differentiated and undifferentiated L6 myoblasts. Lipids. 1978; 13:334–7. [PubMed: 672469]

279. Sahu S, Lynn WS. Lipid composition of human alveolar macrophages. Inflammation. 1977; 2:83–91. [PubMed: 617805]

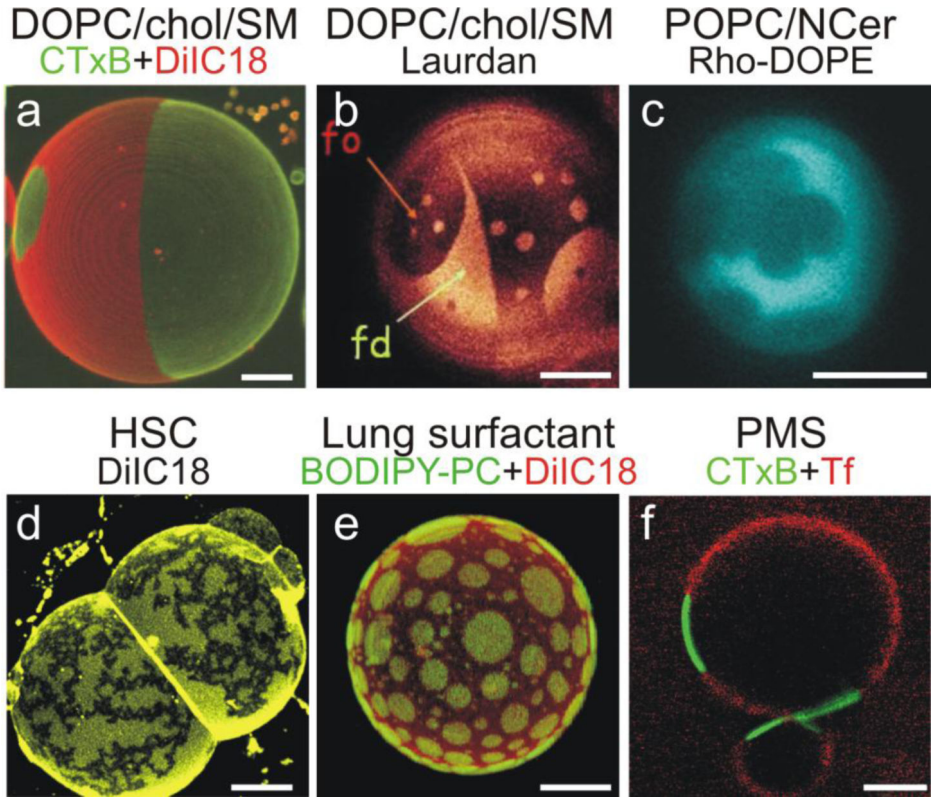

Figure 1. Vizualization of phase coexistence in artificial and very specialized membranes. (a) Giant unilamellar vesicle (GUV) composed of DOPC:cholesterol:SM (1:1:1) and 0.1mol% GM1 Labeling with Alexa 488-CTxB (GM1; green) and DiIC18 (red) and examination at 23°C. **(b) GUV made of DOPC:cholesterol:SM (1:1:1).** Labeling with Laurdan. fo, fluid-ordered; fd, fluid-disordered. **(c) GUV made of POPC and 30% NCeramide mixture.** Labeling with Rhodamine-DOPE and examination at 22°C. (d) Human skin stratum corneum (HSC) lipid membrane. Labeling with DiIC18 and examination at 32°C (*i.e.* skin physiological temperature). **(e) Pig pulmonary surfactant membrane.** Labeling with BODIPY-PC (green) and DiIC18 (red) and examination at 36°C. **(f) PM sphere (PMS) derived from A431 cells.** Labeling with Alexa 488-CTxB (GM1; green) and Alexa 568-transferrin (Tf, red) and examination at 37°C. Notice Lo/Ld (a,b,e,f) *vs* solid-ordered (So)/Ld (c) or So/So (d) phase coexistence. DOPC, 1,2-dioleoyl-*sn*-glycero-3-phosphocholine; POPC, 1-palmitoyl-2-oleoyl-*sn*-glycero-3-phosphocholine; DOPE, 1,2-dioleoyl-*sn*-glycero-3-phosphoethanolamine. All scale bars, 10μm. Adapted with permission from: (a) [17]; (b) [43]; (c) [44]; (d) [18]; (e) [16]; (f) [47].

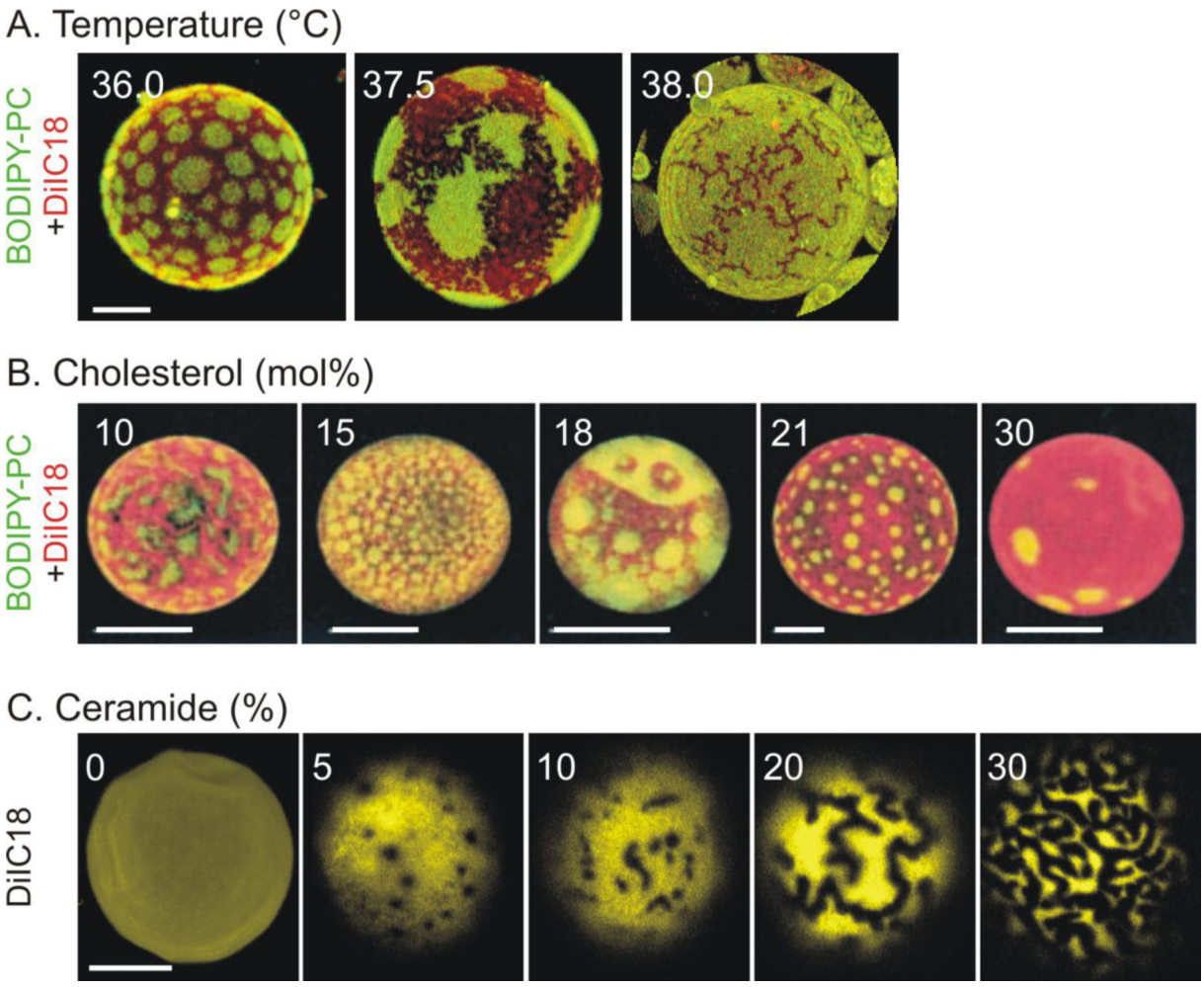

Figure 2. Regulation of phase coexistence in artificial membranes

A. Temperature GUVs of native pulmonary surfactant membranes, labeled with BODIPY-PC (green, Ld) and DiIC18 (red, Lo) and examined at the indicated temperatures. **B. Cholesterol.** GUVs composed of a lipid fraction of pulmonary surfactant membranes at the indicated cholesterol molar ratio, labeled with BODIPY-PC (green, Lo) and DiIC18 (red, Ld) and examined at 25°C. **C. Ceramide (Cer).** GUVs composed of SM:Cer, labeled with DiIC18 and examined at 20°C. All scale bars, 10μm. Adapted with permission from: (A,B) [16]; (C) [61].

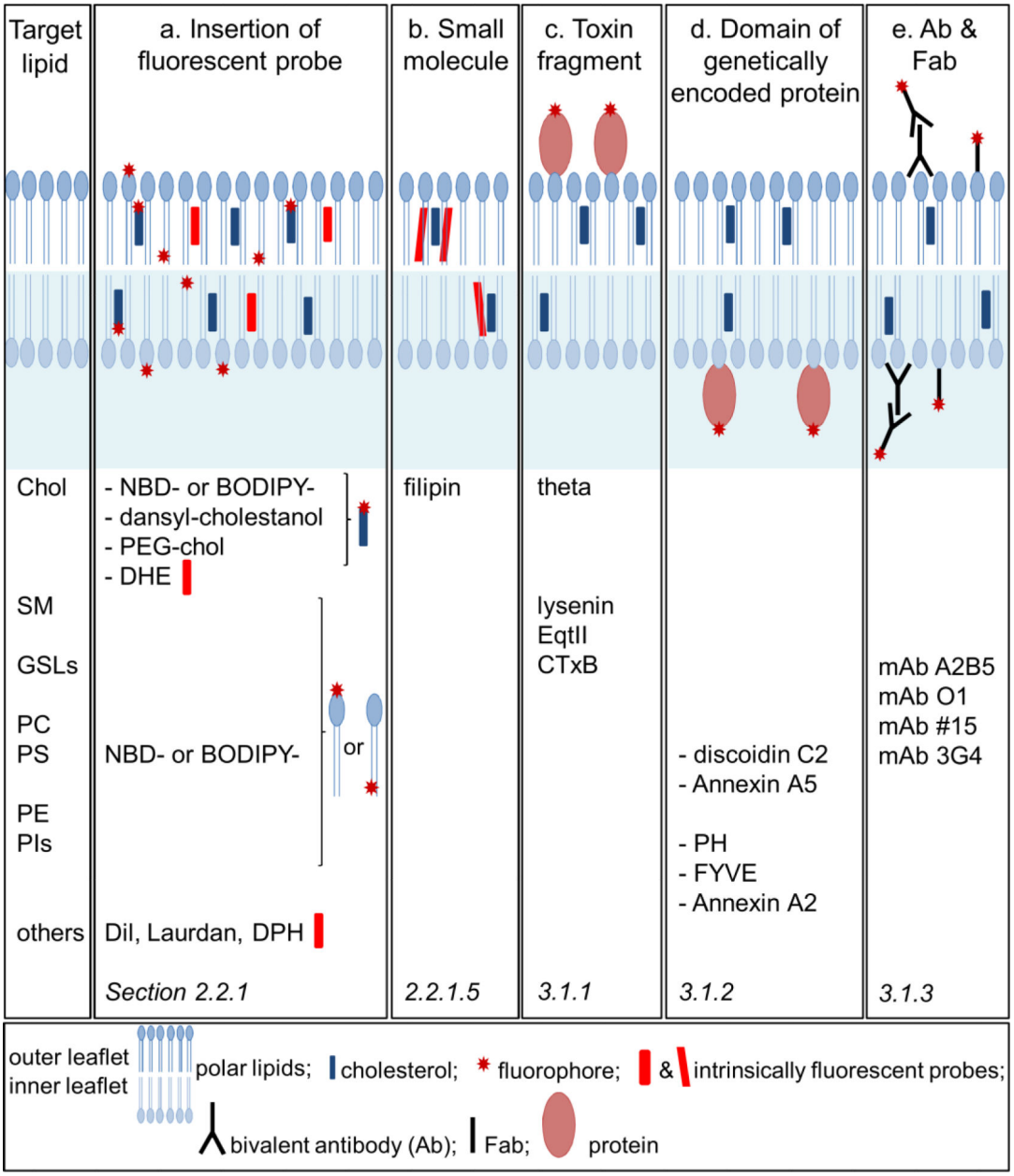

Figure 3. Available tools to visualize lipid organization at the plasma membrane: (a) insertion of exogenous fluorescent lipids; (b-e) decoration of endogenous lipids by exogenous probes

Top, localization of the lipid probes (schematics) in the outer PM (c), inner PM (d), or both leaflets (a [except for PEG-chol in the outer leaflet], b,e). **Bottom,** non-exhaustive listing of mostly used probes. Note that the size of lipids and probes are not to scale. For more information, see text. Chol, cholesterol; EqtII, equinatoxin II; PEG, polyethyleneglycol.

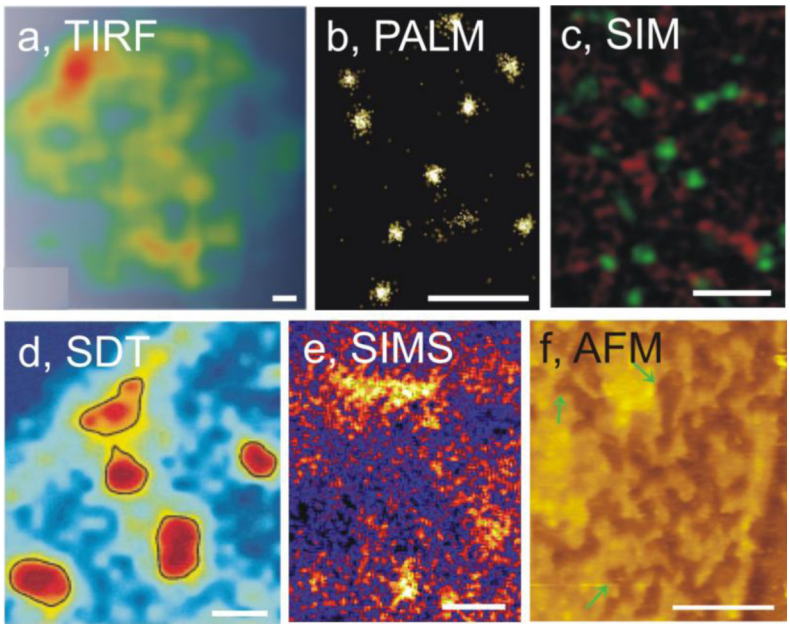

Figure 4. Visualization of plasma membrane lipid submicrometric domains by unconventional diffraction limit microscopy (resolution >200nm; a,b) and higher-resolution microscopy (<200nm; c-f)

(a) Lightguide-based total internal reflection (TIRF) microscopy on HEK293T cells labeled with CTxB. **(b) Photoactivation localization microscopy (PALM)** on HeLa cells labeled with a theta toxin fragment (Dronpatheta-D4). **(c) Structured illumination microscopy (SIM)** at the apical surface of LLC-PK1 cells labeled with equinatoxin (EqtII(8-69)-EGFP; green) and lysenin (mKate-NT-lysenin; red) fragments. **(d) Single Dye Tracing (SDT)** on human airway smooth muscle cells labeled with fluorescent 1,2-dimyristoyl-sn-glycero-3-phosphoethanolamine. (e) Secondary ion mass spectrometry (SIMS) combined with TIRF on fibroblasts labeled with ^{15}N-SL precursors. **(f) Atomic force microscopy (AFM)** on outer PM leaflet of RBC ghosts after cholesterol depletion, which creates indentations (green arrows). All scale bars, 1μm. Adapted with permission from: (a) [145]; (b) [255]; (c) [22]; (d) [114]; (e) [25]; (f) [36].

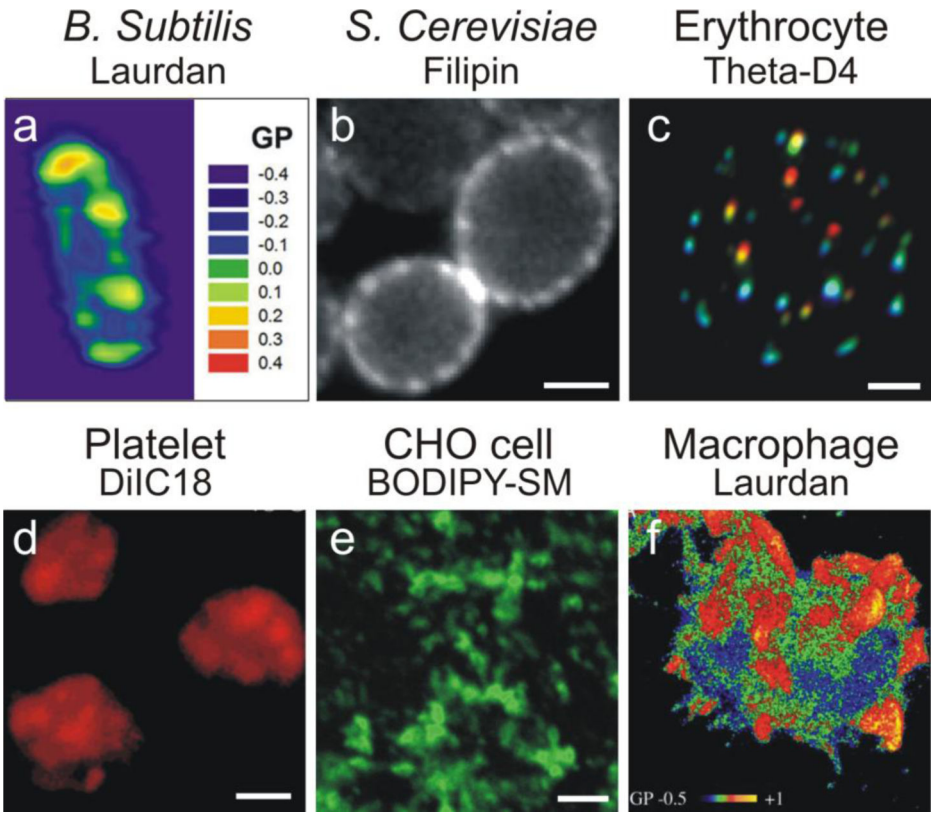

Figure 5. Visualization of plasma membrane lipid submicrometric domains by fluorescence/ confocal vital imaging

(a) *B. Subtilis* labeled with Laurdan at 37°C. **(b) *S. Cerevisiae* stained with filipin**. (c) RBC labeled with theta toxin fragment, mCherry-theta-D4 (cholesterol), at 20°C and examined at the same temperature. **(d) Platelets labeled with DiIC18** and examined at 15°C. **(e) CHO cell labeled with BODIPY-SM**, pretreated with latrunculin B and examined at 4°C (to prevent both endocytosis and membrane protrusions). **(f) Macrophage labeled with Laurdan** and examined at 37°C. All scale bars, 2μm. Adapted with permission from: (a) [31]; (b) [32]; (c) [29]; (d) [91]; (e) [30]; (f) [260].

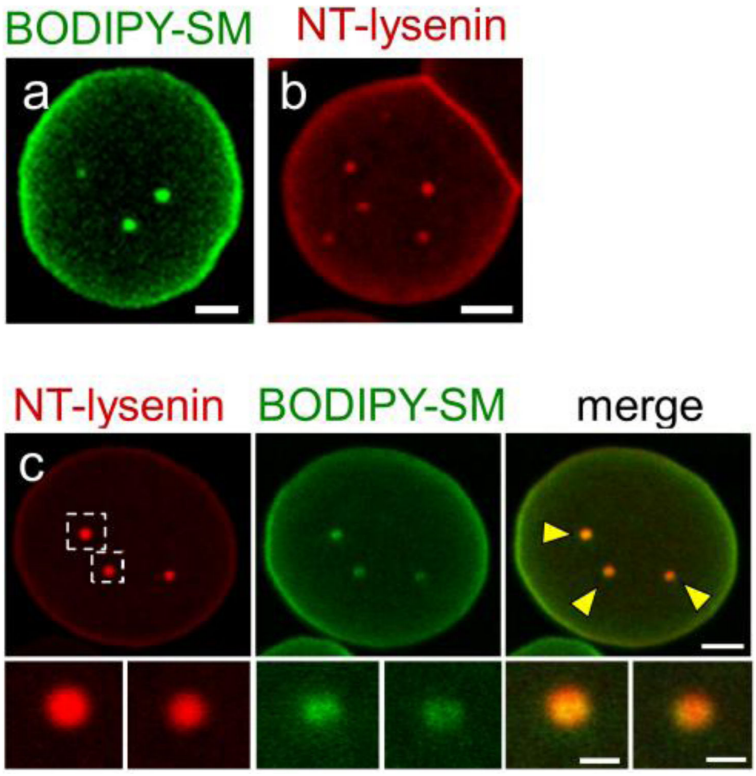

Figure 6. Need to use complementary unrelated probes for a specific lipid: illustration with SM

(a,b) Labeling with either BODIPY-SM (a) or lysenin fragment (b) reveals submicrometric domains. Spread RBCs labeled by insertion of exogenous BODIPY-SM (green) or by lysenin fragment (mCherry-NT-lysenin; red) to decorate endogenous SM and observed at 37°C. (c) Colabeling with BODIPY-SM and lysenin fragment reveals the same domains. Spread RBCs labeled with lysenin fragment, then with BODIPY-SM in the absence of lysenin fragment. Domains boxed at left are enlarged below. All scale bars, 2μm; insets, 1μm. From [26].

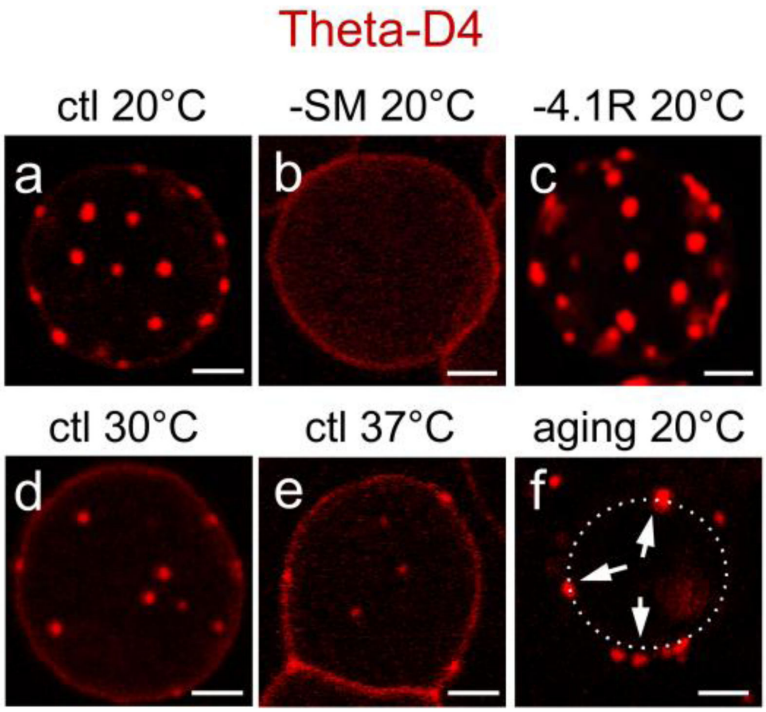

Figure 7. Regulation of plasma membrane lipid submicrometric domains: illustration for cholesterol evidenced with the theta toxin fragment mCherry-theta-D4

(a) Abundance of domains in **control RBC at 20°C**. **(b)** Domain abrogation upon **SM depletion** by sphingomyelinase pre-treatment. **(c)** Increase of domain abundance and size upon acute uncoupling of membrane:cytoskeleton anchorage at 4.1R complexes by PKC activation. **(d,e)** Progressive decrease of domain abundance and size from **20°C** (a) to **30°C** (d) and **37°C** (e). **(f)** Domain expulsion as microvesicles (arrows) upon **accelerated aging** by extended storage at 4°C. Dotted line, RBC profile. All scale bars, 2μm. (a-e) from [29]; (f) unpublished data.

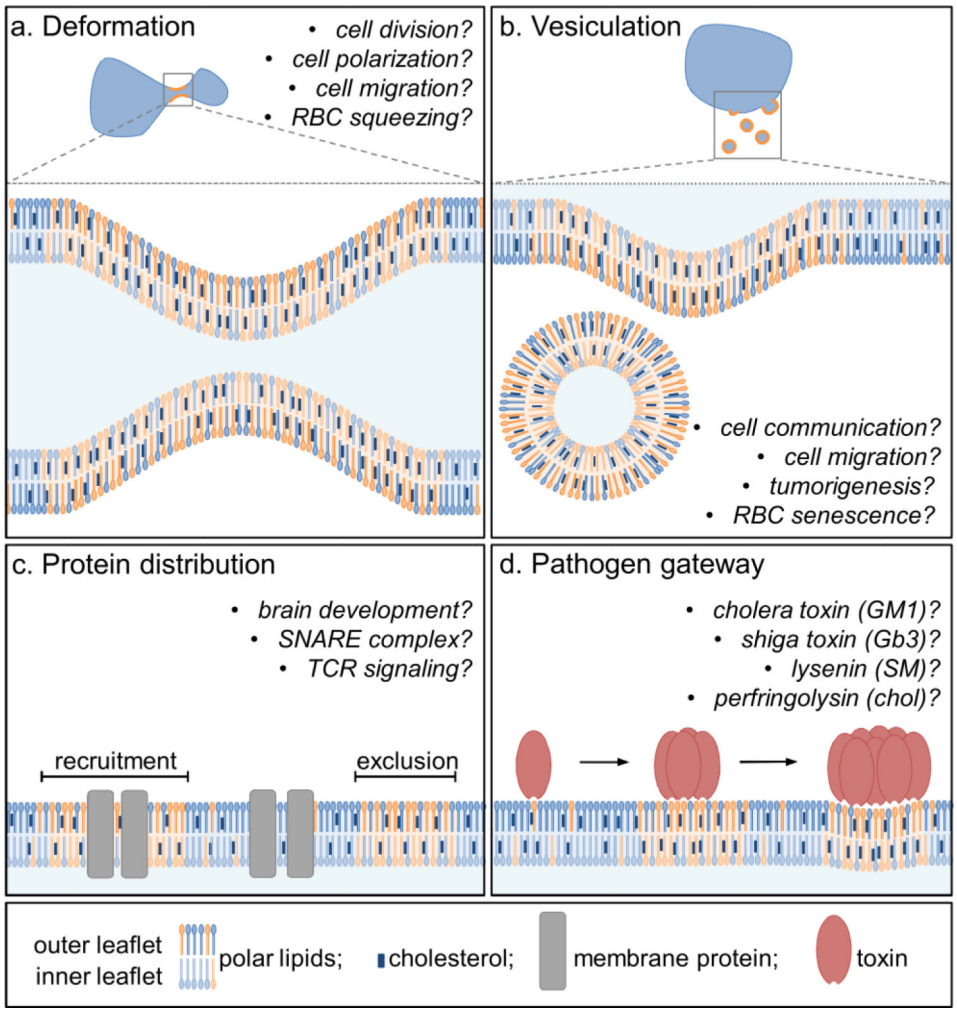

Figure 8. Potential roles for plasma membrane lipid submicrometric domains

For more information, see text. No speculation is made regarding lipid composition of submicrometric domains involved in the different hypothetical roles.

Table 1

Mammalian cells exhibiting plasma membrane submicrometric lipid domains.

Cell	Lipid	Probe	Temperature/fixation	Imaging method	Domain diameter (μm)	Ref.
SPECIFIC LIPID PROBES						
Outer PM leaflet						
Human RBCs	chol	mCherry-theta-D4	10-37°C/living	Confocal	~0.5	[29]
	SM	BODIPY-SM	10-37°C/living	Confocal	~0.5	[30]
		mCherry-NT-lysenin	10-42°C/living	Confocal	~0.5	[26]
	GlcCer	BODIPY-GlcCer	20-37°C/living	Confocal	~0.5	[30]
	GM1	BODIPY-GM1	20°C/living	Confocal	~0.5	[146]
		Alexa 568-CTxB	37°C/living	Confocal	~0.5	[27]
	PC	BODIPY-PC	10-37°C/living	Confocal	~0.5	[146]
		NBD-PC (16:0)	10-37°C/living	Confocal	~0.5	[146]
		NBD-PC (18:1)	10-37°C/living	Confocal	~0.5	[146]
NIH 3T3	SLs	^{15}N-SL precursors	37°C/fixed^{G+O}	SIMS	~0.2	[25]
Human skin fibroblasts	SM	MBP-lysenin	freezen-fracture replica	EM	~0.1	[114]
	LacCer	BODIPY-D-*e*-LacCer	10°C/living	Fluorescence	0.5 - 1 *	[188]
	PC	NBD-PC	18-20°C/living	FRAP	0.35 - 0.5	[19]
CHO	SM	BODIPY-SM	10, 37°C/living	Confocal/FRAP	~0.5	[30]
		NBD-SM	37°C/living	Confocal/FRAP	~0.5	[30]
		NBD-SM	37°C/living	Confocal	>1 *	[173]
	GlcCer	BODIPY-GlcCer	10, 37°C/living	Confocal	~0.5	[30]
	LacCer	BODIPY-D-*e*-LacCer	10°C/living	Confocal	~0.5	[146]
	PC	BODIPY-PC	10°C/living	Confocal/FRAP	~0.5	[146]
C2C12 myoblasts	chol	mCherry-theta-D4	10°C/living	Confocal	~0.5	[29]
HeLa	chol	Dronpa-theta-D4	20°C/fixed^{F}	PALM	~0.24	[22]
	SM	Dronpa-NT-lysenin	20°C/fixed^{F}	PALM	~0.25	[22]
MDCK	GM1	Biotinylated-CTxB	4°C/fixed^{F}	NSOM	0.042 - 0.36	[156]
	GM3	GMR6 antibody	4°C/fixed^{F}	NSOM	0.084 - 0.36	[156]
Endothelial cells	GM1	FITC-CTxB	4°C/fixed^{F}	Confocal	?	[142]
Jurkat cells	SM	HmV-NT-lysenin	4°C/fixed^{F+G+O}	EM	0.12 - 0.16	[24]
	GM3	GM3 antibody	12°C/fixed^{M}	Confocal	>1 *	[135]
	GM1	Biotinylated-CTxB	4°C/fixed^{F+G+O}	EM	0.12 - 0.16	[24]
		FITC-CTxB	12°C/fixed^{M}	Confocal	~1 *	[140]
LLC-PK1	SM	mKate-NT-lysenin	37°C/fixed^{F+G}	SIM	~0.15 - 0.4 *	[114]

Cell	Lipid	Probe	Temperature/fixation	Imaging method	Domain diameter (μm)	Ref.
		EqtII(8-69)-EGFP	37°C/fixed^{F+G}	SIM	~0.2*	[114]
		Alexa 647-lysenin	fixed	PALM/dSTORM	~0.3 - 0.7	[23]
HEK293T	GM1	Alexa 647-CTxB	37°C/living	LG-TIRF	~3	[145]
OLs	GalCer	mGalC IgG3 antibody	fixed^{F}	Confocal	~0.2*	[137]
OL precursors	GM1	Rhodamine-CTxB	4°C/fixed^{F+M}	Confocal	~1*	[179]
	sulfatides	O4 antibody	4°C/fixed^{F+M}	Confocal	>1*	[180]
OL cell line	GalCer	O1 antibody	4°C/fixed^{F}	Confocal	~1*	[178]
	sulfatides	O4 antibody	4°C/fixed^{F}	Confocal	~1*	[178]
PC12	PC	mAb#15 antibody	4°C/fixed^{F}	Confocal	>1*	[134]
Sensory neurons	GM1	Biotinylated CTxB	20°C/fixed^{F}	Fluorescence	>1*	[254]
Inner PM leaflet						
LLC-PK1	PIP_2	Dronpa-PH-PLCδ1	fixed^{F+G}	PALM/dSTORM	~0.3 - 0.7	[23]
OL precursors	PIP_2	GFP-PH-PLCδ1	33°C/living	Confocal	~1*	[175]
NRK	PE	DOPE-Cy3	37°C/living	SDT	0.23 - 0.75	[21]
HASM	PE	DMPE-Cy5	20°C/living	SDT	~0.7	[255]
Both PM leaflets						
L-cell fibroblasts	chol	DHE	37°C/living	Three-photon	?	[143]
ARTIFICIAL LIPID DYES						
Human RBCs		Laurdan	20-37°C/living	Two-photon	0.2-1*	[185, 256-258]
Rabbit RBCs		Laurdan	37°C/living	FCS	0.05 - >0.6	[28]
Human platelets		DiIC18	4-25°C/living	Fluorescence	?	[91]
NIH 3T3		Laurdan	37°C/living	Two-photon/FLIM	>1*	[147]
HeLa		Di-4-ANEPPDHQ	37°C/living	Two-photon	?	[259]
RAW264.7 macrophages		Laurdan	37°C/living	Two-photon	>0.18	[260]
Jurkat cells		DiIC18	37°C/living	Confocal	>1*	[135]
OLs		Laurdan	37°C/living	Two-photon	?	[137]

Cells: CHO, chinese hamster ovary; HASM, human airway smooth muscle; HEK293, human embryonic kidney; HeLa, human cell line derived from cervical cancer; LLC-PK1, pig kidney; MDCK, Madin-Darby canine kidney; NIH 3T3, mouse embryo fibroblast; NRK, normal rat kidney fibroblast; OL, oligodendrocyte; PC12, rat adrenal gland; RBC, red blood cell. **Probes and lipids:** chol, cholesterol; CTxB, cholera toxin B subunit; DHE, dehydroergosterol; DiIC18, dialkylindocarbocyanine C18; Di-4-ANEPPDHQ, a styryl dye; DOPE-Cy3, Cy3-conjugated 1,2-

dioleoyl-sn-glycero-3-phosphoethanolamine; DMPE-Cy5, Cy5-conjugated 1,2-dimyristoyl-sn-glycero-3-phosphoethanolamine; EqtII, equinatoxin II; GalCer, galactosylceramide; GlcCer, glucosylceramide; LacCer, lactosylceramide; MBP, mannose binding protein; PH, pleckstrin homology; PLC, phospholipase C; SL, sphingolipid. **Fixation methods:** F, formaldehyde; G, glutaraldehyde; M, methanol; O, osmium. **Imaging methods:** EM, Electron Microscopy; FCS, Scanning Fluorescence Correlation Spectroscopy; FLIM, Fluorescence Lifetime Imaging Microscopy; FRAP, Fluorescence Recovery After Photobleaching; NSOM, Near-field Scanning Optical Microscopy; PALM, Photoactivation Localization Microscopy; SDT, Single Dye Tracking; SIM, Structured Illumination Microscopy; SIMS, High-resolution Imaging Mass Spectrometry; dSTORM, direct Stochastical Optical Reconstruction Microscopy; LG-TIRF, Lightguide-Based Total Internal Reflection Fluorescence Microscopy.

Domain diameter:

?, size not mentioned by authors.

*domain diameter estimated by ourselves based on image analysis

Table 2

Advantages and limitations of microscopy techniques applied to biological membranes to analyze lipid lateral heterogeneity.

Methods	Advantages	Limitations	Ref.	Figures
HIGH-RESOLUTION CONFOCAL MICROSCOPY AND RELATED TECHNIQUES				
Conventional confocal microscopy	- XY resolution, ~200nm - XZ resolution, ~500nm - live cell imaging & immunofluorescence - possibility of multiple labeling - 3D-reconstruction - easy to use	- photobleaching - phototoxicity - use of fluorescent probes	[261]	Fig.5-7
Two-photon excitation	- deep imaging into the sample - focal vertical excitation - limited photodamage - visualization of UV-excited probes	- XY resolution twice lower than confocal - use of fluorescent probes	[43]	Fig.5a
Total Internal Reflection Fluorescence (TIRF)	- XZ resolution, ~100nm - limited photodamage - negligible background noise	- restriction to interface between two media of specific refraction index - use of fluorescent probes	[262]	Fig.4a
Fluorescence Recovery After Photobleaching (FRAP)	- dynamics of lateral diffusion and compartmentalization	- photobleaching - diffusion properties of a pool of molecules - use of fluorescent probes	[263]	--
Fluorescence Lifetime Imaging Microscopy (FLIM)	- high temporal resolution - possibility to gain information of environment (viscosity, lipid:lipid and lipid:protein interactions)	- difficult analysis of molecules with multiple lifetime - complex and cost equipment - use of fluorescent probes	[264]	--
Fluorescence Correlation Spectroscopy (FCS)	- molecular concentration measurement - diffusion measurement - possibility to study molecular interactions - possibility of combination with several imaging methods	- use of highly-photostable fluorescent probes	[265]	--
SUPER-RESOLUTION MICROSCOPY				
PhotoActivated Localization Microscopy (PALM) & Stochastic Optical Reconstruction Microscopy (STORM)	- single molecule imaging - XY resolution, ~20nm - XZ resolution, ~50nm	- general requirement of sample fixation - use of fluorescent probes - slow image acquisition for mobile molecules - high photodamage - potential blur during the overall recording time	[266]	Fig.4b
Structured Illumination Microscopy (SIM)	- XY resolution, ~100nm	- sample fixation - lengthy image acquisition - specialized hardware system	[267]	Fig.4c
Single Dye Tracing (SDT)	- high temporal resolution - single molecule diffusion properties	- heavy computational system - use of fluorescent probes	[268]	Fig.4d
SECONDARY ION MASS SPECTROSCOPY				
Secondary Ion Mass Spectrometry (SIMS)	- study of endogenous molecule - XY resolution, ~50-100nm - possibility of data quantification	- sample fixation - requirement of ultra-high vacuum	[269]	Fig.4e
SCANNING PROBE MICROSCOPY				
Atomic Force Microscopy (AFM)	- XY resolution, ~10nm - study of endogenous molecule - topography analysis - measurement of mechanical properties (deformation and elasticity)	- tip-sample distance challenge - tip fragility - complex data analysis	[154]	Fig.4f

Methods	Advantages	Limitations	Ref.	Figures
	- measurement of molecular interactions (chemical or hydrophobic adhesion and receptor-ligand interaction)			
Near-Field Scanning Optical Microscopy (NSOM)	- XY resolution, ~20-100nm - topography analysis	- lengthy image acquisition - challenging for live imaging - use of fluorescent probes	[155]	--

For details, see text.

Table 3

Lipid composition of the plasma membrane of different cells.

Molar %	Polar lipids								Sterols[a]	Other	Ref.
	PC	PE	PI	PS	PA	PG	CL	SLs[a]			
E. coli		82		traces		6	12				[157, 270]
S. cerevisiae	25	10	9	3	5		2	10-20 *MIPC*	30-40 *erg*		[157, 271, 272]
Human RBCs	24	6	traces	3	traces			19 *SM*	48 *chol*	traces	[90, 157]
Human platelets	18	20	1	12				16 *SM*	32 *chol*		[273, 274]
Fibroblast cell line (NIH 3T3)	43	16	8	6.5	1.5			12 *SM*	13 *chol*		[275]
Chinese hamster ovary cells (CHO)	25	21	n.d.	7				12 *SM*	35 *chol*		[276]
Schwann cell line (NF1T)	27	9	6	2				18 *SM*	38 *chol*		[277]
Undifferentiated L6 myoblasts	24	9	2	6				16 *SM*	42 *chol*		[278]
Human alveolar macrophages	30	21		21				7 *SM*	8 *chol*	13	[157, 279]

PC, phosphatidylcholine; PE, phosphatidylethanolamine; PI, phosphatidylinositol; PS, phosphatidylserine; PA, phosphatidic acid; PG, phosphatidylglycerol; CL, cardiolipin; SLs, sphingolipids; MIPC, mannosyl-inositol phosphorylceramide; SM, sphingomyelin; erg, ergosterol; chol, cholesterol.

n.d., not detected.

[a]The most abundant lipid of these categories is indicated in italic.